Tunnelling and Underground Space Technology 130 (2022) 104734

Contents lists available at ScienceDirect

Tunnelling and Underground Space Technology incorporating Trenchless Technology Research

journal homepage: www.elsevier.com/locate/tust

Numerical analyses of twin stacked mechanized tunnels in soft grounds – Influence of their position and construction procedure

Ngoc Anh Do [a,*], Daniel Dias [b], Mohammad-Reza Baghban Golpasand [c], Van Kien Dang [a], Ouahcène Nait-Rabah [e], Van Vi Pham [a], Trong Thang Dang [d]

[a] Hanoi University of Mining and Geology, Faculty of Civil Engineering, Hanoi, Viet Nam
[b] Grenoble Alpes University, Laboratory 3SR, Grenoble, France
[c] Department of Civil Engineering, Seraj Institute of Higher Education, Tabriz, Iran
[d] Vietnam Institute for Building Science and Technology – IBST, Hanoi, Viet Nam
[e] UMR EcoFoG, Université de Guyane, Kourou, France

ARTICLE INFO

Keywords:
Twin stacked tunnel
Numerical modelling
Lagging distance
Pillar depth
Settlement
Structural forces

ABSTRACT

Twin stacked tunnels become more and more common due to the limited surface area and underground space. Most researchers have already paid attention separately to the influence of the twin stacked tunnels' position and construction sequence. However, the influence of the lagging distance and pillar depth of twin stacked tunnels has not yet been fully investigated when considering the tunnels construction sequence. The present study aims at analysing the effect of the construction sequence, pillar depth between tunnels, and lagging distance between stacked tunnels' faces on the structural forces induced in the tunnel linings and on the surface settlements. For this purpose a three-dimensional (3D) numerical model was developed using the finite difference element code FLAC^{3D}. Most of the parameters of the slurry-type shield machine were simulated. The analyses included the influence of the face support pressure, shield conicity, shield weight, grouting pressure, harden grout, jacking forces, the weight of the backup train and jointed segmental lining. The results indicated that the most critical scenario, both in terms of ground settlement and internal forces in the tunnel lining is when the upper tunnel (UT) is excavated first and followed by the lower tunnel (LT) excavation. On the other hand, the following upper tunnel should be excavated at a lagging distance, which is larger by about 4 to 5 times the tunnel diameter behind the preceding lower tunnel. The research results reviled that designing a too small pillar depth between stacked tunnels should be avoided. This concerns pillar depths of about 0.25 to 0.5 times the tunnel diameter, as indicated in this study. It could cause a great increment in the normal displacements, longitudinal forces, and bending moments in the lower tunnel lining.

1. Introduction

Twin tunnels located at shallow depth in soft ground conditions are a good solution well adapted to rapid development and expansion of urban cities. They are usually excavated in horizontal parallel profiles, but recently tunnels that stacked over each other became more common due to the limited surface area and underground space. In the case of stacked tunnels, the distance between tunnels' centres is designed as short as possible to reduce the entire tunnel's length. Previous engineering experiences and studies available in the literature reviled that the lining of an existing tunnel and surrounding soil can be greatly affected by the construction of overlapped tunnels (Do et al., 2014a; Liu et al. 2021). The influence between stacked tunnels could not, therefore, be neglected to ensure safe construction process.

The interaction between the twin tunnels has been reviewed in recent publications (Kim, 2004; Chapman et al., 2007; Yang et al., 2017; Do et al., 2014b; Soomro et al., 2021a; Zhang et al., 2020; Islam and Iskander, 2021; Zhou et al., 2021; Chortis and Kavvadas, 2021). Islam and Iskander (2021) presented a review of twin tunneling-induced surface settlements. The paper begins with an overview of volume losses, and factors affecting settlements above twin tunneling. A summary of the effects of the construction sequence, clear distance between tunnels, and cover depth has then been introduced for four twin tunneling scenarios including (i) horizontally parallel, (ii) stacked, (iii)

* Corresponding author at: Hanoi University of Mining and Geology, Faculty of Civil Engineering, Hanoi, Viet Nam.
E-mail address: nado1977bb@gmail.com (N.A. Do).

https://doi.org/10.1016/j.tust.2022.104734
Received 22 October 2021; Received in revised form 1 August 2022; Accepted 28 August 2022

perpendicularly crossing, and (iv) inclined arrangement twin tunneling. Based on the review of over 200 case studies, the authors concluded that the twin tunnels behavior and induced ground settlements are usually thoroughly studied for side-by-side twin tunnels and to some extent for stacked tunnels. However, further investigations are needed to properly understand the mechanism of stacked tunnels interactions. In particular, particular attention needs to be paid to the time delay between staggered twin stacked tunnels construction and the pillar depth, when considering the construction works execution effect.

A number of interesting researches on twin stacked tunnels can be found in available literature (Addenbrooke and Potts, 2001; Hefny et al., 2004; Mo and Chen, 2008; Chapman et al., 2007; Do et al., 2014a; Senthilnath and Velu, 2016; Yang et al., 2017; Boon and Ooi, 2018; Fang et al., 2020; Yang et al., 2020; Soomro et al., 2020; Soomro et al., 2021b; Do et al., 2021; Islam and Iskander, 2021). Addenbrooke and Potts (2001), based on the numerical results of twin stacked tunnel construction, indicated that the settlement profile above the second tunnel is distinctly different in shape from an equivalent greenfield profile, regardless of the construction sequence. The distortion and displacement of the existing lining are greater if the second tunnel passes beneath rather than above the existing tunnel. Do et al. (2014a) performed a numerical investigation of two stacked tunnels' construction sequences impacting the tunnels' interaction and the surrounding ground. They indicated that the worst possible condition is when the upper tunnel is firstly excavated and followed by the lower tunnel earth works. The same finding was given by Boon and Ooi (2018). Yang et al. (2017) analyzed deformations and internal forces of a power tunnel lining existing above twin overlapped tunnels excavated below using both physical model experiments and numerical simulations. The effects of different construction sequences and tunneling time framework were highlighted. The results indicated that the case when the lower tunnel is constructed first is safer than when beginning with the upper tunnel in terms of internal forces and settlements of the existing tunnel. Yang et al. (2020) used a three-dimensional numerical model to study the influence of the overlapped tunnel excavation sequences on the ground movements and tunnel lining behavior. By comparing the effects of the two excavation scenarios on the ground and tunnel lining, they recommended that the excavation should be carried out considering firstly the lower tunnel followed by the upper tunnel. In Islam and Iskander (2021), it is concluded that the ground settlements are smaller when the cover depth is larger. The smaller the clearer the distance between tunnels is and the flatter the settlements trough above the tunnel centerline are. A new tunnel excavation work executed above an existing tunnel often causes upheavals. When the new tunnel is excavated underneath the existing upper tunnel, the interaction always occurs and the existing upper tunnel settles. The tunneling sequence where the upper tunnel is excavated at first leads to higher settlements. Fang et al. (2020) numerically investigated the vertical soil displacements induced by fully stacked tunnels, constructed using tunnel boring machines. The results showed that the ultimate maximum settlement value is more affected by the construction of the upper tunnel than by the lower tunnel. The zone of the ground settlement profile over the twin stacked tunnels is only affected by the lower tunnel. Do et al. (2021) investigated the influence of the shield machine operation parameters, such as the face support pressure, grouting pressure, and shield's length during twin stacked tunnel excavation, on the surface settlements using 3D finite difference elements calculations. The results indicated that an increase in the grouting pressure and face pressure did not always cause a decrease in surface settlements. The length and conicity of the shield machine have a strong effect on the surface settlements.

Most published works to date paid attention mainly to the influence of twin stacked tunnels construction sequence, and shield operation parameters. However, the influence of the lagging distance and pillar depth of twin stacked tunnels is not yet fully investigated when considering the tunnels construction sequence.

During the construction of twin, tunnels excavated close to each other, the horizontal lagging distance between tunnels' faces has a significant effect on the behavior of tunnels and surrounding soils (Ng et al., 2004; Zhang et al., 2010; Do et al., 2016; Tang et al., 2016). Ng et al. (2004) conducted a numerical analysis of side-by-side tunnels excavated using the New Austrian Tunneling Method. They found that the lagging distance has a significant effect on the lateral movements than on the tunnels vertical displacements. Lagging distance also caused a change in the internal forces of each tunnel, especially at the opposite sides of tunnels. Zhang et al. (2010) performed a centrifugal model test to explore the longitudinal deformation range of the preceding tunnel influenced by unloading caused by the stacked following tunnel, using the conventional excavation method. The results stated that the differential displacements of the preceding tunnel induced by the following tunnel mainly occurred in a range between 3.5D (diameter) ahead and 3.0D behind the excavation face of the following tunnel. Do et al. (2016) investigated the interaction between twin mechanized side-by-side tunnels. The numerical results indicated that the change of the bending moment and the lining displacements in twin tunnels are generally opposite, depending on the lagging distance of tunnel faces. All three researches focused on the case of twin horizontally parallel tunnels. The influence of the lagging distance between stacked tunnels' faces on their behavior was not studied at all. Tang et al. (2016) conducted a 3D numerical analysis on the effect of the vertical distance between stacked tunnels and investigated the lagging distance role on soil deformation and tunnel lining behavior. The results showed that a reasonable lagging distance between tunnels depends on the vertical clear spacing between stacked tunnels. The greater the clear spacing, the higher the distance. It should be noted that stacked tunnels were constructed using the conventional NATM method in this work.

In this study, 3D finite-difference models (FDM) were built to investigate six different scenarios of twin stacked mechanized tunnels by changing the excavation sequence of the upper and lower tunnels, and their pillar depth. Most performance parameters of the mechanized tunneling process were simulated. Particular attention was paid to the influence of the horizontally lagging distance between tunnels' faces when considering the change in the construction sequences and the pillar depth between the upper and lower tunnels. The variation of displacements and structural forces of the tunnel linings and movements of surrounding soils depending on the construction scenarios were highlighted. The effective construction sequence, the pillar depth between tunnels, and the critical lagging distance between stacked tunnels' faces were also presented.

2. Numerical model

2.1. Modelling mechanized tunnelling process

For the purpose of the present study, the tunneling conditions of the Bologna-Florence high-speed railway line project in Italy, (ring 582), were adopted (Do et al., 2014a; Do et al., 2014b). The excavation process of tunnels was simulated by the explicit finite difference method (FDM) FLAC^{3D}. Tunnels with an external diameter of 9.4 m excavated by the slurry-type shield machine and supported by a segmental lining with a thickness of 0.4 m were considered. Each lining ring is 1.5 m wide and includes 6 segments which are staggered and assembled in the longitudinal tunnel direction (Figs. 1, 2).

All numerical calculations were conducted in a homogeneous soil profile applying drained conditions. The soft soil was modeled using the Cap-Yield (CYsoil). It is a strain-hardening constitutive model that is defined by a frictional Mohr-Coulomb shear envelope (zero cohesion) and an elliptic volumetric cap in the (p', q) plane (Itasca, 2013). The CYsoil model takes strain-dependent soil stiffness into account and appropriately represents the behaviour of soft soils and the unloading/loading condition during tunnelling works. Numerical models of drained triaxial tests were simulated in order to calibrate the CYsoil constitutive model parameters using the input data of the Bologna-Florence tunnel

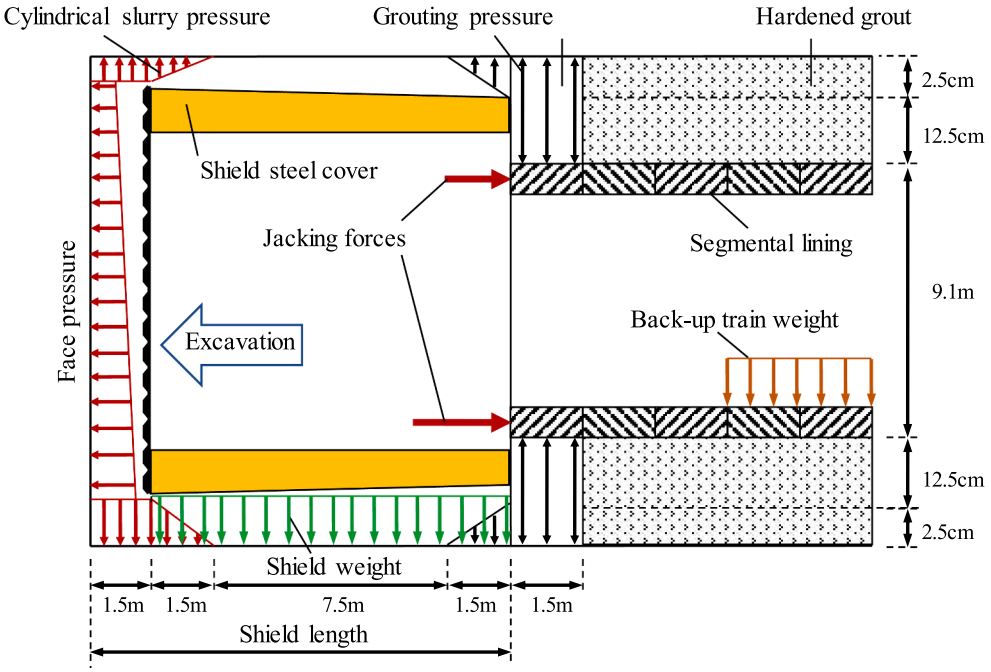

Fig. 1. Modelled components of the shield machine (not scaled).

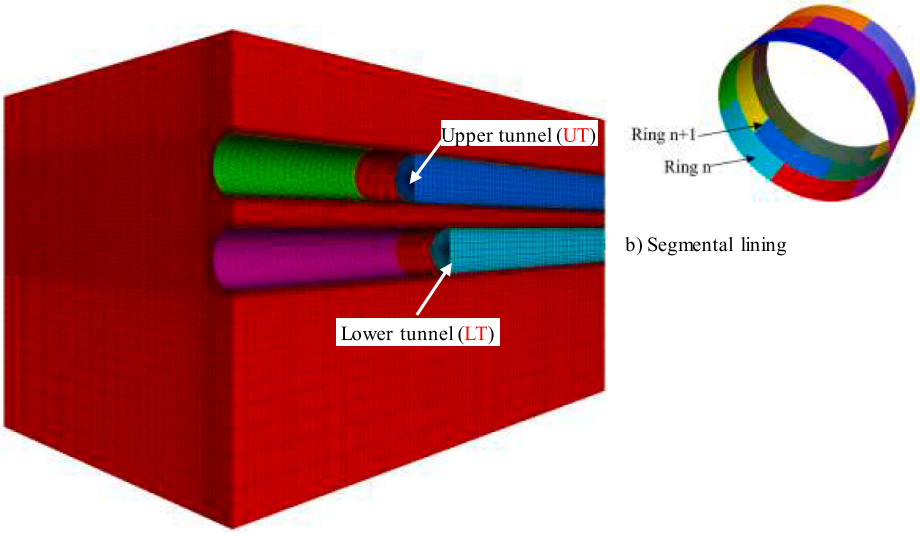

Fig. 2. Scheme of the numerical model used in the study.

project (Do et al., 2014c). The input soil parameters used in the modeling are summarized in Table 1.

The 3D numerical model is based on the works of Do et al. (2014a; 2014b). The most important excavation processes of a mechanized tunneling work using a shield machine are simulated (see Fig. 1). The shield has been implicitly modeled as a "virtual" shell, i.e., grid points surrounding the "virtual" shield will be artificially fixed during the soil displacement when they get in contact with the "virtual" shield (Mollon et al., 2012). The shield's self-weight of 6000 kN is simulated by considering the vertical loads applied on the grid points in a range of 90 degrees at the shield's bottom area and 12 m over the shield length (Fig. 1) (Do et al., 2014a; Do et al., 2014b).

The face pressure is simulated by a trapezoidal distribution with a pressure gradient of 11 kPa to consider the slurry density. The face pressure value at the tunnel spring line was estimated as dependent on the horizontal stress ahead of the tunnel's face (Mollon et al., 2012). Because of a slight overcutting, an additional pressure applied to the cylindrical surface just behind the tunnel face is also simulated. The grouting pressure at the shield tail applied both on the exterior of the last

Table 1
Soil's parameters (Do et al., 2014b).

CYsoil model	Value
Reference elastic tangent shear modulus G^e_{ref} (MPa)	58
Elastic tangent shear modulus G^e (MPa) $G^e = G^e_{ref}(\sigma_3/p^{ref})$	98
Elastic tangent bulk modulus K^e (MPa) $K^e = K^e_{ref}(\sigma_3/p^{ref})$	213
Reference effective pressure p^{ref} (kPa)	100
Failure ratio R_f	0.9
Ultimate friction angle ϕ_f (degrees)	37
Calibration factor β	2.35
Lateral earth pressure factor K_o	0.5

lining ring and the tunnel boundary, is modelled by a gravitationally controlled distributed load, increasing over the tunnel height to take into consideration the grout unit weight effect. The grouting pressure value at the tunnel crown is 1.2 times the vertical soil pressure, as recommended by Do et al. (2014b). As the injected grout dries quickly, the grout is assumed to be hard enough after the installation of one lining ring (1.5 m as shown in Fig. 1) (Epel et al., 2021). Beyond this length, hardened grout was simulated through the volume elements characterized by a perfectly elastic behavior. The elastic characteristics of the grout layer are $E_{grout} = 10$ MPa and $\nu_{grout} = 0.22$. This simple simulation of the grout is adopted in the present paper because it has already been successfully used in previous validated numerical analyses (Dias and Kastner, 2012; Mollon et al., 2012).

A linear distribution increasing from the top to the bottom of the tunnel is assumed to model the jacking forces applied over the tunnel height. The jacking forces acting on the lining segments are determined based on Rijke (2006) and are represented by forces applied directly on the nodes located at the segment's front edge, installed behind the shield. The backup train which weights 3980 kN is modelled through a distribution loading applied on the segmental lining's bottom area over an assumed angle of 90 degrees and along a tunnel length of 72 m behind the shield tail (Do et al., 2014a; Do et al., 2014b) (Fig. 1).

Following Do et al. (2014b), Do et al., (2016) and Epel et al. (2021), the segmental lining is simulated by linear-elastic embedded liner elements. Embedded liner elements have two links at each node allowing both the lining-zone interaction and connection between lining segments. It means that one link of the embedded liner element is connected to the surrounding soil, and the other link allows connecting to adjacent segments. The lining-zone connection is assumed to be linear-elastic and is modelled by a stiffness (Do et al., 2014a; Itasca, 2013) in which the normal stiffness and tangential stiffness are set equal to one hundred times the equivalent stiffness of the stiffest neighbouring zone. The stiffnesses of the joints between segments in a ring are modeled by a rotational spring (K_θ), an axial spring (K_A), and a radial spring (K_R). On the other hand, the rigidity of the connection between successive rings is simulated by a set of a rotational spring ($K_{\theta R}$), an axial spring (K_{AR}), and a radial spring (K_{RR}) (Do et al., 2014a; Do et al., 2014b). More details on joint stiffness are given in the works of Thienert and Pulsfort (2011) and Do et al. (2014a).

The tunnel construction was sequentially simulated based on a step-by-step procedure. The procedure was implemented using Fish codes (Flac internal programming language) considering the following steps:

- Step 1: Tunnel excavation for a lining ring width (i.e., 1.5 m) and installation of the segments of the new lining ring;
- Step 2: Applying simultaneously the shield weight's forces, face pressures, grouting pressures, jacking forces, and backup train forces to the tunnel and surrounding soils in the newly excavated section. Hardening of the grout elements surrounding the 2nd lining ring counted from the shield tail;
- Step 3: Solving the model to reach equilibrium;
- Step 4: Starting the next cycle by removing the pressures and forces assigned at Step 2;
- Repeating the 1–4 steps.

2.2. Scenarios considered for the twin stacked tunnel excavation

The proposed numerical model (section 2.1) is used to model two typical construction sequences of twin stacked tunnels, i.e., (1) the lower tunnel is excavated first and followed by the upper tunnel (LT-UT case), and (2) the upper tunnel is excavated first and followed by the lower tunnel construction (UT-LT case). Figs. 3 and 4 illustrate cases where the lower tunnel is excavated first. In practice, the first construction sequence is usually chosen due to the advantages of reducing the adverse interaction between stacked tunnels and surface settlements (Boon and Ooi, 2018; Do et al., 2014a; Yang et al., 2017; Yang et al., 2020). The case where the upper tunnel is excavated first is not widely used but considered in this study for comparison purposes.

To investigate the lagging distance effect between the twin stacked tunnels' faces on the soil movements and lining behavior, six scenarios were analyzed by changing the pillar depth (clear vertical distance) between the upper tunnel's bottom and the lower tunnel's crown (B value in Figs. 3 and 4) and the tunnels construction sequence (Table 3). Scenarios 1, 2, and 3 where the lower tunnel is excavated first were adopted with B values of 0.25D, 0.5D, and 1D, respectively. Meanwhile, scenarios 4, 5, and 6 correspondingly illustrate the cases when the upper

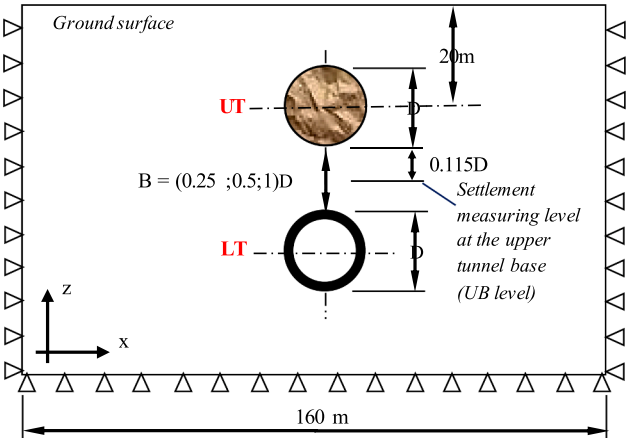

Fig. 4. Typical cross-section (A–A) view of the twin stacked tunnels (not scaled).

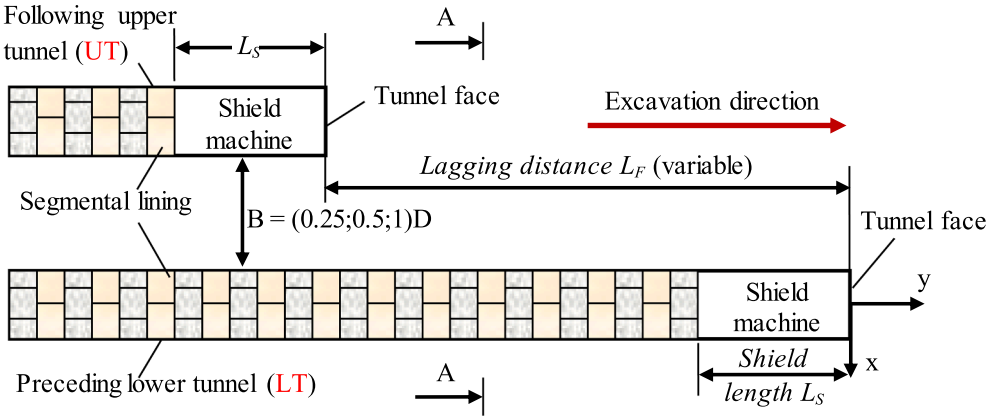

Fig. 3. Longitudinal view of the twin stacked tunnels in scenarios 1, 2, and 3 (not scaled).

Table 3
Investigated scenarios of twin stacked tunnels.

Scenario	Name	Depth to the upper tunnel's center (m)	Pillar depth (D)	Depth to the lower tunnel's center (m)	First tunnel	Second tunnel
1	LT-UT_0.25D	20 (2.1D)	0.25D	31.75 (3.4D)	LT	UT
2	LT-UT_0.5D		0.5D	34.1 (3.6D)	LT	UT
3	LT-UT_1D		1D	38.8 (4.1D)	LT	UT
4	UT-LT_0.25D		0.25D	31.75 (3.4D)	UT	LT
5	UT-LT_0.5D		0.5D	34.1 (3.6D)	UT	LT
6	UT-LT_1D		1D	38.8 (4.1D)	UT	LT

tunnel is excavated first with B values of 0.25D, 0.5D, and 1D. Addenbrooke and Potts (2001) and Koungelis and Augarde (2004) stated that the interaction between stacked tunnels is negligible when the pillar depth (B) is greater than 1D when the lower tunnel is excavated first. It means that the interaction effects between tunnels are negligible for a pillar distance (B) of 1D. Thus, the behaviour of both upper and lower tunnels is independent. However, when the upper tunnel is excavated first, the interaction effect should be considered regardless of the lower tunnel depth. As mentioned above, the case where the upper tunnel is excavated first is not common and is just studied here for comparison purposes. Therefore, the case where pillar depth (B) is larger than 1D is not considered in this study.

The lagging distance influence between stacked tunnels is considered in scenarios 1, 2, 3, and 6. In scenarios 4 and 5, which rarely occur due to the short vertical distance between the preceding (first) upper tunnel and the following (second) lower tunnel, only the case in which the following lower tunnel is constructed far behind the preceding upper tunnel is analyzed. It should be noted that in all these six scenarios, the upper tunnel position is fixed at the depth of 20 m (2.1D), measured from the ground surface to the tunnel's center.

In scenarios 1, 2, 3, and 6, six lagging distance L_F cases between the preceding tunnel and the following tunnel were simulated: $0L_S$, $1L_S$, $2L_S$, $3L_S$, $4L_S$, and $6L_S$. L_S is the shield machine length ($L_S = 12$ m) (Figs. 2 and 3). The case $L_F = 0L_S$ means that the two tunnels are parallelly excavated at the same time. The case of $L_F = 1L_S$ corresponds to a scenario when the following tunnel face is at the same shield tail transverse section of the preceding tunnel. The case $L_F = 6\ L_S$ assumes that the following tunnel is constructed when the preceding tunnel has reached a steady state. In total, 26 numerical calculations were conducted considering (1) tunnel excavation sequence, (2) pillar depth between tunnels (B), and (3) horizontal lagging distance between the tunnels' faces (L_F). All the numerical calculations were conducted without considering the underground water presence.

A parametric study was conducted to eliminate the boundary condition effects. Accordingly, while the width of the 3D model was set to 160 m, the length and height of models varied depending on the scenarios of the center-to-center distance of tunnels and horizontal lagging distance between tunnels' faces. To avoid the boundary conditions influence, a monitored section of the structural forces and displacements of the lining and movements of the surrounding soils were taken at a distance of about 5D from the boundary. The excavation of the following tunnel is ended when the following tunnel passed the monitored section at a minimum distance of 5D.

3. Numerical results and discussion

In each numerical calculation, settlements and lateral movements of the soil, structural forces, and displacements induced in the tunnel linings are presented. In addition, the results of twin stacked tunnels are compared with those of a corresponding single upper or a single lower tunnel to highlight the tunnels' interaction impact. The results were determined at the cross-section of the 33rd ring of the following tunnel, counting from the model boundary (y = 0 m), to eliminate the influence of the boundary condition (Do et al., 2014a; Do et al., 2014b). The location of this ring corresponds to the distance of about 5D measured from the boundary in the y-direction.

3.1. Settlements

During the excavation of twin stacked tunnels, the following tunnel is excavated within the soil mass which is disturbed by the preceding tunnel. Depending on the horizontal lagging distance and the vertical pillar depth between tunnels, the redistribution process of stresses and strains in the soil mass surrounding the preceding tunnel is taking place. Therefore, the development of deformation and internal forces induced in the preceding tunnel lining could reach the ultimate state or could take place when the following tunnel's face is reaching the initial section. Hence, it is important to simultaneously investigate the vertical soil deformations in the longitudinal direction and the cross-section of the tunnel.

Fig. 5 presents the transverse settlement trough on the ground surface, above the single tunnel and the twin stacked tunnels. The following tunnel is excavated when the preceding tunnel works are completed. Fig. 6 and Table 4 illustrate the maximum surface settlement developed in the single tunnel case and 6 scenarios of twin stacked tunnels, where the following tunnel is constructed far behind the preceding tunnel, ($L_F = 6L_S$ regardless of the lagging distance). Table 4 also presents the volume loss ratios determined as the ratio of the settlement along and the cross-section area of a tunnel. Fig. 7 shows the influence of the horizontal lagging distance (L_F) on the maximum surface settlement for scenarios 1, 2, 3, and 6. For comparison purposes, the settlement troughs developed over the single tunnel at different corresponding depths are also presented.

Figs. 5, 6, and Table 4 indicate that an increase in the depth of a single tunnel results in a significant surface settlement decrease. The deeper the single tunnel, the shallower and flatter the settlements (Fig. 5). The result is in good agreement with the numerical results obtained by Hejazi et al. (2008). Indeed, the maximum surface settlements over a single tunnel are 0.128 %D, 0.142 %D, 0.148 %D, and 0.204 %D when the single tunnel depths are, respectively, 4.1D, 3.6D, 3.4D, and 2.1D. Nevertheless, the volume loss ratios of the three deeper tunnel cases are nearly constant (0.84–0.85%), while for shallower tunnels the value is 0.72% (Table 4). It means that in this study, a deeper tunnel results in a larger volume loss ratio, but at a depth that is high enough, the volume loss ratio is almost constant.

After the construction of the second tunnel, a great increase of the settlements is observed (Figs. 5, 6). However, the ultimate maximum settlement value is more affected by the excavation of an upper tunnel than by the excavation of a lower tunnel. In other words, the construction sequence has a significant influence on the maximum surface settlement. Indeed, the scenarios where the new lower tunnel is excavated underneath the existing upper tunnel cause smaller settlements than in the case where the upper tunnel is excavated first. The relative differences (S_{LU}/S_{UL}) from 89.3% to 86.4% are noted when the pillar depth (B) changes from 0.25D to 1D (Fig. 6 and Table 4). This could be attributed to the fact that, firstly, the following (second) tunnel is excavated through the strained soil mass caused by the excavation of the preceding (first) tunnel, the supplementary settlement induced by the second tunnel is therefore always smaller compared with the developed settlement when this tunnel is excavated first in an undisturbed zone. Secondly, as seen in Figs. 5 and 6, the settlement resulting from the deeper tunnel is always smaller than the one caused by the shallower tunnel. Consequently, the total settlement above the twin stacked

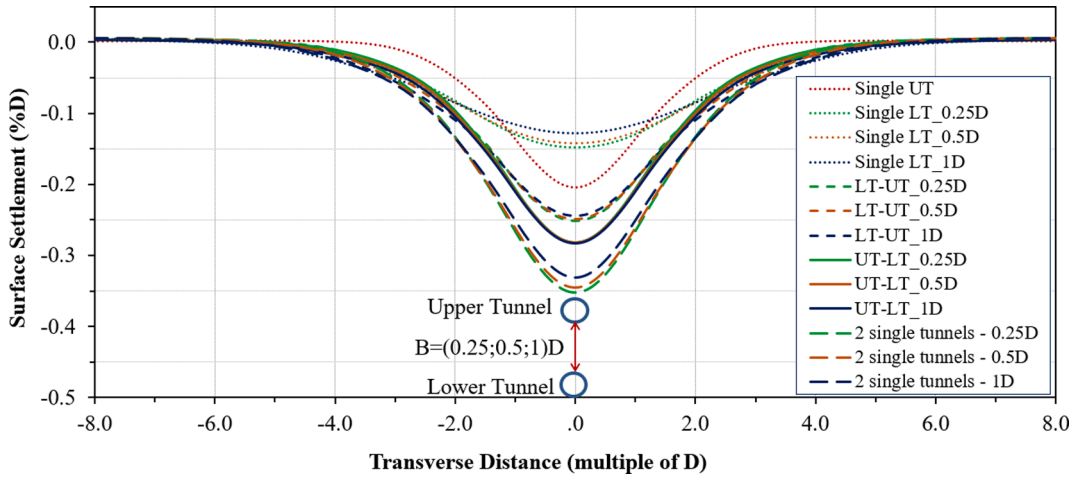

Fig. 5. Surface settlement troughs in the transverse section of the single tunnel and twin stacked tunnels ($L_F = 6L_S$).

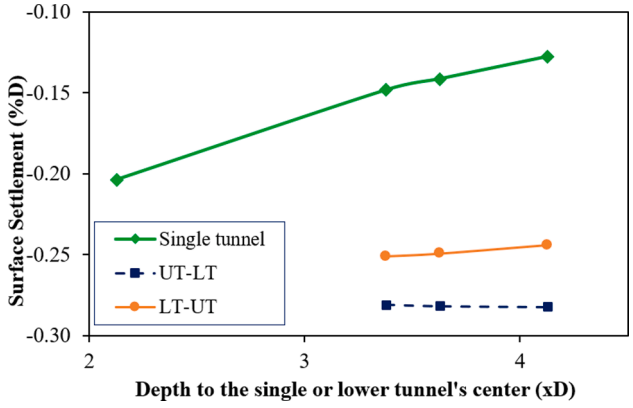

Fig. 6. Maximum surface settlements above the single tunnel and twin stacked tunnels ($L_F = 6L_S$).

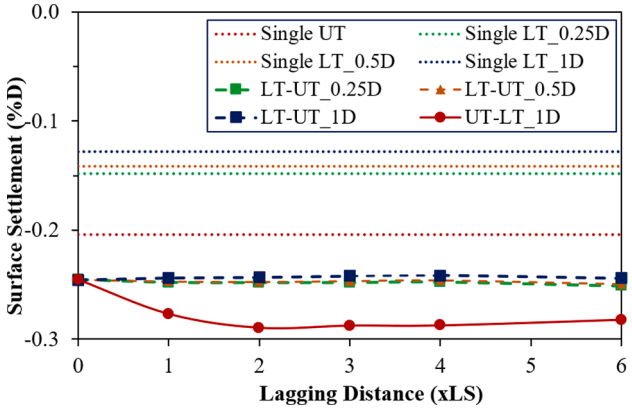

Fig. 7. Maximum surface settlements above the single and twin stacked tunnels depending on the L_F distance.

Table 4
Maximum surface settlement above single tunnel and twin stacked tunnels ($L_F = 6L_S$).

Scenario	1 or 4	2 or 5	3 or 6
Depth to the lower tunnel's center (D)	3.4	3.6	4.1
	Maximum surface settlement (%D)/ Volume Loss (%)		
Single LT (S_L)/(V_L)	−0.148 / 0.84	−0.142 / 0.84	−0.128 / 0.85
Single UT (S_U)/(V_U)	−0.204 / 0.72		
LT-UT (S_{LU})/(V_{LU})	−0.251 / 1.14	−0.249 / 1.17	−0.244 / 1.24
UT-LT (S_{UL})/(V_{UL})	−0.281 / 1.19	−0.282 / 1.23	−0.282 / 1.27
S_{LU}/S_L (%)	169.2	176.2	191.1
S_{UL}/S_U (%)	137.9	138.3	138.5
S_{LU}/S_{UL} (%)	89.3	88.5	86.4
2 Single tunnels (S_{2S})/(V_{2S})	−0.352 / 1.537	−0.345 / 1.538	−0.332 / 1.554
S_{2S}/S_{LU} (%)	140.24	138.55	136.07
S_{2S}/S_{UL} (%)	125.27	122.34	117.73

tunnels when the lower tunnel is excavated first is smaller than when the upper tunnel is excavated first. This is consistent with Fang et al. (2020), Hage Chehade and Shahrour (2008), Channabasavaraj and Vishwanath (2012), and Do et al. (2014a).

It is interesting to note that the settlement trough width over the lower tunnels is similar to the twin stacked tunnels in most scenarios and is wider than for the single upper tunnel case (Fig. 5). This implies that the settlement trough width over twin stacked tunnels is sustainably related to the lower tunnel and is nearly independent on the tunnels' construction sequences. The construction of the following upper tunnel in scenarios 1, 2, and 3 does not further widen the settlement trough existing over the preceding upper tunnel. The reason could be due to the fact that the lower tunnel causes a wider settlement trough. This finding is consistent with monitored and numerical results obtained by Fang et al. (2020). It is reasonable to conclude that during twin stacked tunnels construction, while the maximum settlement is strongly dependent on the upper tunnel, the settlement trough width is however influenced by the lower tunnel. Table 4 indicates that the volume loss ratios observed in scenarios 1, 2, and 3 are slightly smaller than those of scenarios 4, 5, and 6.

To highlight the effect of the preceding tunnel on the following tunnel, the sum of the settlements caused by two single tunnels for 3 cases of the distance between 2 tunnels of 0.25D, 0.5D and 1D are introduced in Fig. 5. In addition, the corresponding values of the maximum surface settlement (S_{2S}) and volume loss (V_{2S}) are presented in Table 4. The results indicate that settlements caused by twin tunnels cannot be regarded as simply the sum of the two single tunnels. Indeed, the sum of settlements and volume loss caused by the two single tunnels are always higher than the corresponding values of twin tunnels. As mentioned above, the reason could be explained by the soil mass movements surrounding the following (second) tunnel caused by the excavation of the preceding (first) tunnel. The closer the tunnels'

distance is, greater the effect of the preceding tunnel on the strained soil mass surrounding the following tunnel is. Thus, the settlement induced by the second tunnel is always smaller than if the tunnel was excavated in an undisturbed zone. The smaller pillar depth (B) induced the higher difference between the sum of the settlements caused by the two single tunnels and that of twin tunnels, represented by larger ratios of S_{2S}/S_{LU} and S_{2S}/S_{UL} (Table 4).

Fig. 6 and Table 4 also show that when the upper tunnel is excavated first, the construction of the following lower tunnel leads to a relative increase of the maximum settlement (S_{UL}/S_U) of about 138% and is nearly independent on the tunnels pillar depth. Nevertheless, in the cases where the lower tunnel is excavated first, the excavation of the following upper tunnel causes a greater increase in the maximum settlement (S_{LU}/S_L) from 169.2% to 191.1%, depending on the tunnels pillar depth (Table 4). It means that the lower–upper stacked tunnel construction sequence is more dependent on the tunnels pillar depth than on the upper-lower tunnel construction procedure. The same conclusion was obtained through the numerical study of Koungelis and Augarde (2004). The reason is connected to the effect of the first upper tunnel, which can be considered as a reinforcement above the second lower tunnel excavated later. It simply limits the supplementary settlement caused by the lower tunnel construction (Li and Yuan, 2012). Additionally, due to the effect of the preceding tunnel excavation on the soil mass surrounding the following tunnel, Fig. 6 indicates that the tunnel depth has a greater influence on the settlements induced over a single tunnel than by twin stacked tunnels, represented by the steeper line.

It is interesting to note (Fig. 7) that the greater the lagging distance (L_F) between tunnels' faces, the larger the maximum surface settlement over twin tunnels. This could be explained by the fact that the settlement developed during tunneling is a time-depending process and change in distance measured from the tunnel face. Normally, the settlement of a single tunnel reaches a steady-state at a distance of 3D to 5D behind the tunnel face (Do et al., 2014a). Hence, settlements above the first tunnel are more completely developed before the construction of the second following tunnel when the lagging distance increases. In other words, greater lagging distance often leads to larger settlements caused by the first tunnel, and therefore to total settlements over twin tunnels. The differences in terms of maximum settlements caused by the lagging distance in scenarios of upper-lower and lower–upper tunnel construction sequences (Fig. 7) are smaller than 15.0% and 2.34%, respectively. It is therefore reasonable to conclude that the lagging distance influence on the maximum settlement above twin stacked tunnels when the lower tunnel is excavated first could be neglected, in particular for pillar depths of 1D. This conclusion is clearly shown when considering the longitudinal settlements (Fig. 9) described below. In scenario 6 where the lower tunnel is excavated underneath the existing upper tunnel at a pillar depth of 1D, the lagged tunnel construction procedure always causes a greater settlement in comparison with the twin tunnels excavated in concurrent configuration (Fig. 7).

To highlight the impact of the interaction between stacked tunnels in terms of vertical soil movements, Figs. 8, 9, and 10 illustrate the longitudinal settlement profiles developed at the ground surface when the second tunnel is excavated after finishing the first tunnel construction and in scenarios 3 and 6 when considering the lagging distance (L_F) change. Meanwhile, Figs. 11, 12, and 13 present the longitudinal upheaval/settlement profiles rising at the upper tunnel base level in the single and twin stacked tunnels cases and in scenarios 3 and 6 with different lagging distances, respectively. Other results of longitudinal settlements for scenarios 1 and 2 when considering the lagging distance effect are also determined. It allows obtaining nearly the same recommendation as for scenario 3. It should be mentioned that the longitudinal settlements determined at the upper tunnel base are measured at a distance of 0.115D below the tunnel's bottom (UB level in Fig. 4).

Fig. 8 shows a considerable influence of the twin stacked tunnels' construction sequence on the longitudinal settlement profiles slope. For the case of a single tunnel, a deeper tunnel leads to a smaller ultimate settlement and also a smaller longitudinal settlement profile around the tunnel face area. Like the research results indicated in Fig. 5 and Table 4, Fig. 8 shows an increase of the surface settlements for twin stacked tunnels compared to the single tunnel case. In scenarios 1, 2, and 3, when the lower tunnel is excavated first, the ultimate longitudinal settlement profile at the ground surface (dashed lines) is shallower but steeper at the following tunnel's face than those of scenarios 4, 5, and 6 (dotted lines) (Fig. 8). It could be explained by the great effect of the settlement induced by the upper tunnels which are excavated afterward. It is interesting to mention that, in scenarios 4, 5, and 6, the influence of the following lower tunnel on the ultimate longitudinal settlement profile is independent on the tunnels pillar depth. The reinforcement effect of the existing upper tunnel during the construction of the lower tunnel can explain such influence. In addition, the distance behind the following tunnel face at which settlement reaches the ultimate state is about 3.5D in scenarios 4, 5, and 6. It is longer than the influenced distance of about 2D in scenarios 1, 2, and 3 (Fig. 8). In other words, the longitudinal settlement development is completed sooner behind the tunnel face in scenarios 1, 2, and 3 when the lower tunnel is excavated first.

When the upper tunnel is staggered and excavated behind the lower tunnel, a greater lagging distance (L_F) between the tunnels' faces is followed by a smaller longitudinal settlement profile (Fig. 9 for scenario

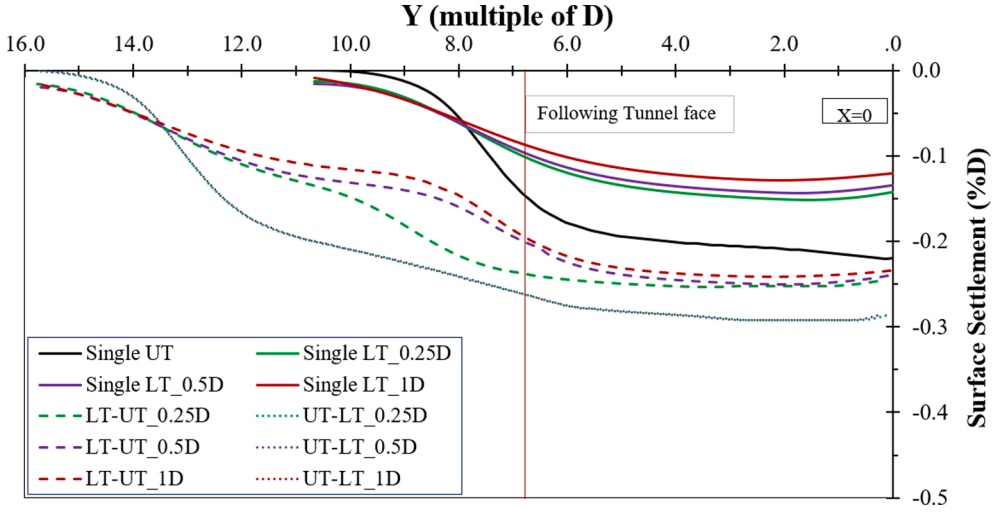

Fig. 8. Longitudinal settlement profiles at the ground surface above the single tunnel and twin stacked tunnels.

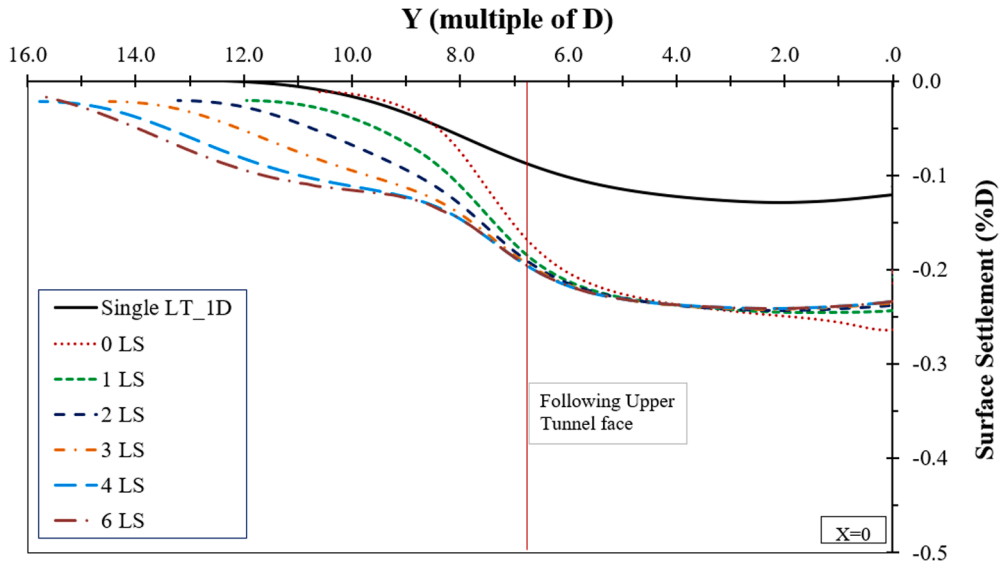

Fig. 9. Longitudinal settlement profiles at the ground surface in scenario considering the change in lagging distance L_F.

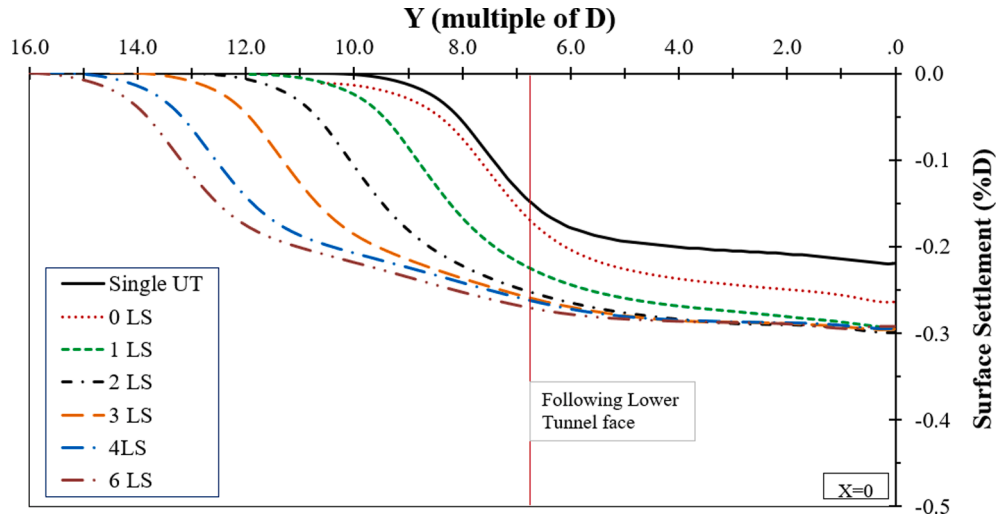

Fig. 10. Longitudinal settlement profiles on the ground surface in scenario 6 considering the change in lagging distance L_F.

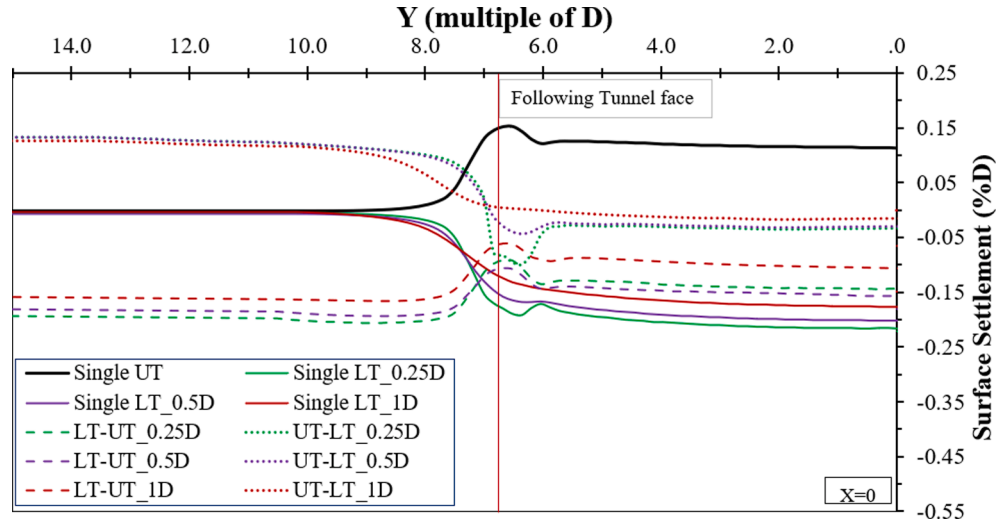

Fig. 11. Longitudinal settlement profiles at the upper tunnel base in the case of single tunnel and twin stacked tunnels.

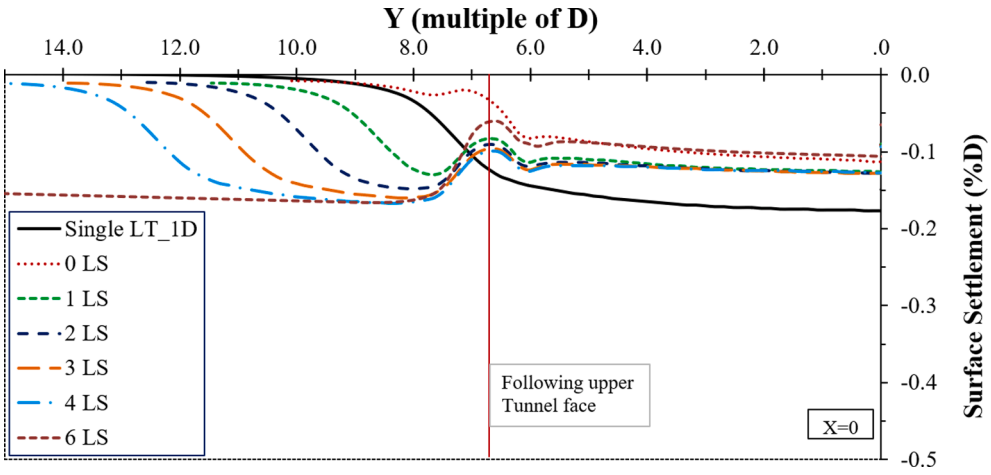

Fig. 12. Longitudinal settlement profiles (uplift movement) at the upper tunnel base in scenario 3 considering the change in lagging distance L_F.

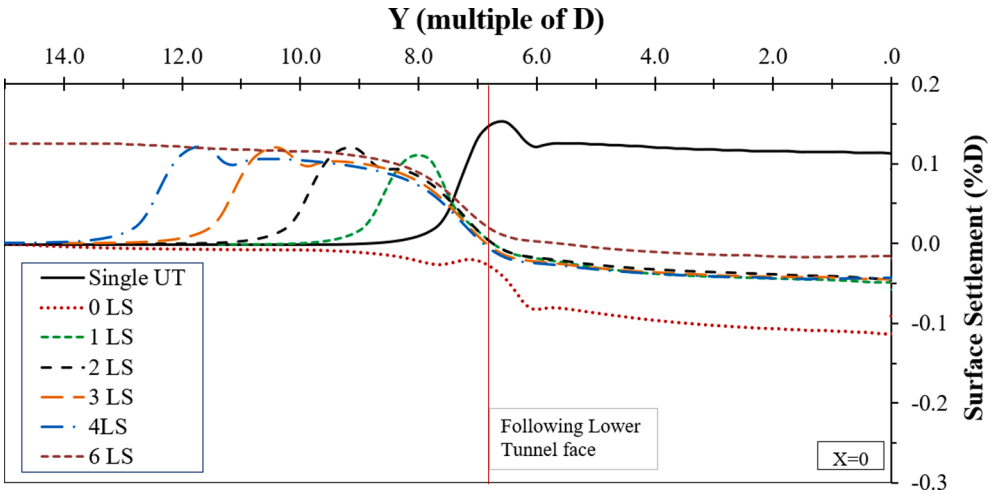

Fig. 13. Longitudinal settlement profiles at the upper tunnel base in scenario 6 considering the change in lagging distance L_F.

3). The case where twin tunnels are excavated concurrently leads to the steepest longitudinal settlements. Fig. 9 also shows that the tunnel faces lagging distance has an insignificant influence on the surface settlement at the cross-section of the following upper tunnel face and the ultimate settlement over twin tunnels. It is due to the smaller impact of the lower tunnel construction on the surface settlement in comparison with the shallower upper tunnel. The same observations are obtained in numerical results of scenarios 1 and 2.

Unlike the results obtained in scenarios 1, 2, and 3, Fig. 10 illustrates a larger difference in the surface settlements measured at the cross-section of the following lower tunnel face constructed behind the upper tunnel (scenario 6) depending on the lagging distance (L_F). A shorter lagging distance causes a smaller surface settlement measured at the section of the following lower tunnel face. The smallest instantaneous surface settlement is observed when two tunnels are excavated concurrently. This could be explained by the accumulation of both the longitudinal settlement effects caused by the upper and the lower tunnels. At a smaller lagging distance, the longitudinal settlements developed over the preceding upper tunnel are still under development when the following lower tunnel faces passing through. Therefore, the settlement accumulation caused by both tunnels decreases when the lagging distance decreases (Fig. 10). Furthermore, it should be noted that a smaller lagging distance will cause a steeper longitudinal settlement profile. However, the ultimate settlements over twin tunnels are nearly similar and independent of the lagging distance, excepting the case where two tunnels are excavated concurrently ($L_F = 0$).

The longitudinal settlement profiles determined at the upper tunnel base (UB level in Fig. 4) introduced in Fig. 11 indicate a great upheave of the vertical soil displacements caused by (1) the shield machine process, i.e., face pressure, grouting pressure, conicity of the shield, and (2) gravity effect. Due to the face excavation, progressive relaxation of the strains induced ahead the tunnel face could be predicted. Right after the tunnel face, an increase of the vertical soil movements appears because of the shied machine overcutting (Mollon et al., 2012). Behind this movement, a slight increase of the vertical soil displacements along the shield is related to its conicity. At the tunnel base and along the shield, because of the shield weight which causes downward movements against the upheaval ones resulting from the shield conicity, a small settlement can be anticipated. The grout pressure injected into the void behind the shield tail induces an upheave. Along with the tunnel section behind the shield tail, soil movements are dependent on gravity. Because of the low lateral earth pressure coefficient ($K_0 = 0.5$) in the present study, while the soil above the tunnel tends to move downwards to the tunnel, the soil at the tunnel bottom usually upheaves.

Using the above analysis of the shield performance and gravity acting on the soil movements, an upheaval movement ahead the tunnel face for the single upper tunnel base (UB level) is seen (Fig. 11). This is due to the gravity effect and face excavation mentioned above which cause soil displacements towards the tunnel face. A slight settlement is observed because of the equivalence between the opposite effects of the

conicity and the shield weight at the tunnel base. For the deeper single tunnel, for instance, in the case of the tunnel's center depth of 3.4D (single lower tunnel_0.25D case), the decompressive movement and gravity action cause a significant settlement ahead of the tunnel face. The soil is then considerably upheaved after the grouting pressure impact. Behind this part, the soil settles due to the consolidation process. When the tunnel depth continues to increase, settlements measured at the UB level decrease due to the larger distance from the tunnel crown to the measured (UB) level (Fig. 11).

In scenario 1, when the lower tunnel is excavated first and followed by the upper tunnel with a small pillar depth of 0.25D (Fig. 11), the upheaval movement induced close to the following upper tunnel face, is due to the gravity effect and face excavation. It is then followed by a significant settlement under the grouting pressure impact at the tail of the upper shield. Fig. 11 indicates that, in scenarios 1, 2, and 3, the successive excavations of the following upper tunnel result in an uplift of the soil above the lower tunnel. The uplift amount is dependent on the vertical distance between tunnels. Smaller tunnel pillar depth usually leads to a greater uplift effect induced in the lower tunnel. Subtracting the settlements at the ultimate state of the twin tunnels by the ones induced after finishing the first lower tunnel construction gives an uplift movement of 0.073 %D, 0.061 %D, and 0.059 %D corresponding to scenarios 1, 2, and 3. This finding is consistent with Addenbrooke and Potts (2001).

In contrast to scenarios 1, 2, and 3, the excavation of the following lower tunnel underneath the preceding upper tunnel results in a supplementary settlement. By subtraction of the settlement measured at the UB level of the single upper tunnel from the one measured after the construction of the following tunnel in scenarios 4, 5, and 6, Fig. 11 shows an additional settlement at the UB level of 0.16 %D, 0.148 %D, and 0.122 %D for pillar depth cases of 0.25D, 0.5D, and 1D, respectively. It implies that a larger vertical distance between tunnels is followed by a smaller supplementary settlement caused by the following lower tunnel affecting the upper tunnel.

Regarding the lagging distance effect, Fig. 12 indicates an insignificant impact on the uplift movements, caused by the excavation of the following upper tunnel in scenario 3, at small lagging distances. Indeed, at shorter lagging distances (L_F) of $1L_S$, $2L_S$, $3L_S$, and 4 L_S which means

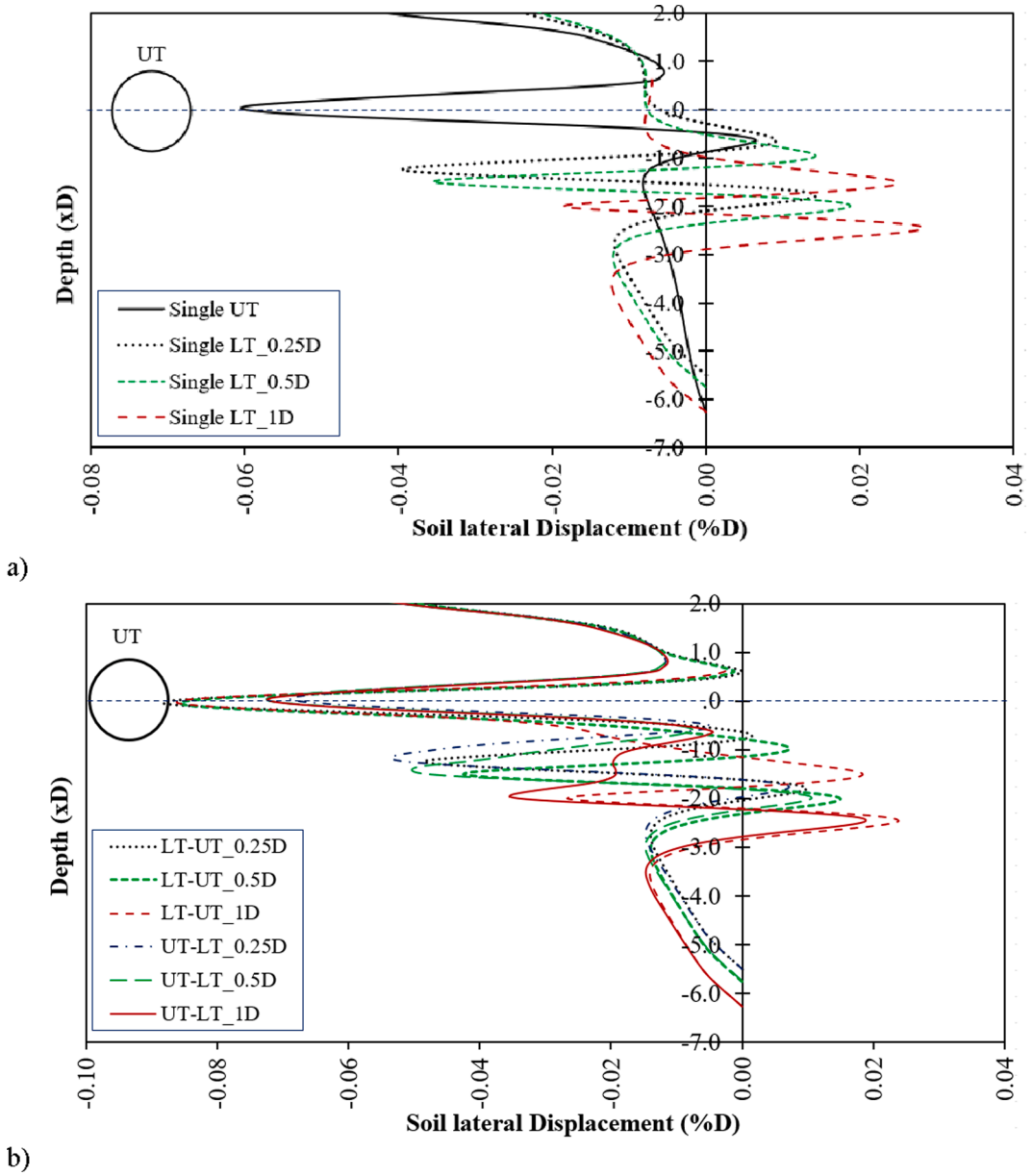

Fig. 14. Lateral displacements induced in the soil along the TS axis of (a) single tunnel and (b) twin stacked tunnels ($L_F = 6L_S$).

that the following upper tunnel face is closer to the preceding lower tunnel face, the uplift behavior is less important due to the downward soil movement caused by the lower tunnel excavation. This movement is still under development and therefore leads to an upward movement decrease in the soil above the lower tunnel. The largest uplift behavior is observed when the upper tunnel is excavated after the lower tunnel construction (Fig. 12). At that time, downward movements over the lower tunnel are null.

Fig. 13 shows a great influence of the lagging distance between tunnels on the supplementary settlement below the preceding upper tunnel caused by the excavation of the following lower tunnel (scenario 6). The smallest settlement increment at the UB level is seen when the lower tunnel is excavated after the first upper tunnel construction. It is because the upward soil movements at the preceding upper tunnel bottom, induced by the effect of low lateral earth pressure coefficient ($K_0 = 0.5$), were fully developed. As a result, downward movements below the upper tunnel base and above the lower tunnel excavated later will be reduced when the lagging distance increase as presented in Fig. 13.

3.2. Soil lateral displacements

Regarding the lateral soil displacements, Fig. 14 shows the movement profiles measured after the excavation of the single tunnel and twin stacked tunnels. The TS axis is positioned on the right side and at a distance of 1.25*D* from the tunnels' center. The negative lateral displacements mean that the ground is moving towards the tunnel side. The results in this figure are only for the cases in which the following tunnel is excavated when the preceding tunnel is finished. The relationship between the maximum lateral soil movements and the excavation scenarios is presented in Fig. 15 and Table 5. The influence of the lagging distance between tunnels' faces on ground lateral movements is introduced in Fig. 16.

Figs. 14, 15, and Table 5 show the inward movement of the soil close to the spring line towards the tunnel. This is attributed to the significant stress release of the soil surrounding the tunnel (Soomro et al., 2020; Soomro et al., 2021b). The same observation is also indicated in previous research (e.g., Surjadinata et al., 2005; Loganathan, 2009; Basile, 2014; Wang et al., 2017). In the case of a single tunnel, the shallower tunnel is, the greater lateral soil displacements toward the tunnel side are. The dependence is nearly linear (Fig. 15). The excavation of the following tunnel causes lateral soil movements to increase at the existing tunnel's spring line which results in further release of soil stress induced by the second tunnel (Soomro et al., 2021b). In addition, lateral soil movements at the spring line of the upper tunnel are always greater than the spring line ones of the lower tunnel for all twin stacked tunnels scenarios. In comparison with the single upper tunnel, while the lower–upper tunnel procedure, i.e., scenarios 1, 2, 3, leads to a great increase in the lateral soil movements (from 142 to 146 %), smaller

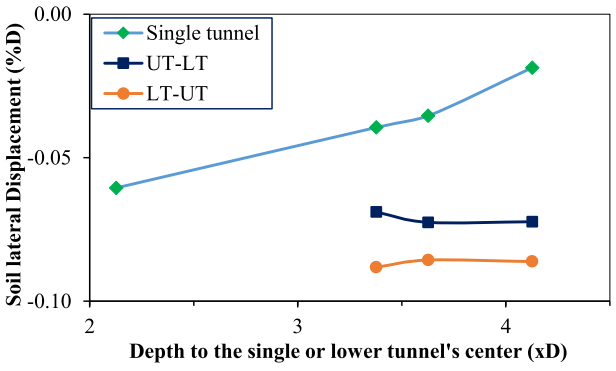

Fig. 15. Soil's maximum lateral displacements along the TS axis of the single tunnel and twin stacked tunnels ($L_F = 6L_S$).

Table 5
Maximum lateral soil movement along TS axis in single tunnel and twin stacked tunnels ($L_F = 6L_S$).

Scenario	1 or 4	2 or 5	3 or 6
Depth to the lower tunnel's center (D)	3.4	3.6	4.1
	Maximum lateral soil movement (%D)		
Single LT (X_L)	−0.039	−0.035	−0.019
Single UT (X_U)	−0.061		
LT-UT (X_{LU})	−0.088	−0.086	−0.086
UT-LT (X_{UL})	−0.069	−0.073	−0.072
X_{LU}/X_U (%)	146	142	142
X_{UL}/X_U (%)	114	120	120
X_{LU}/X_{UL} (%)	128	118	119

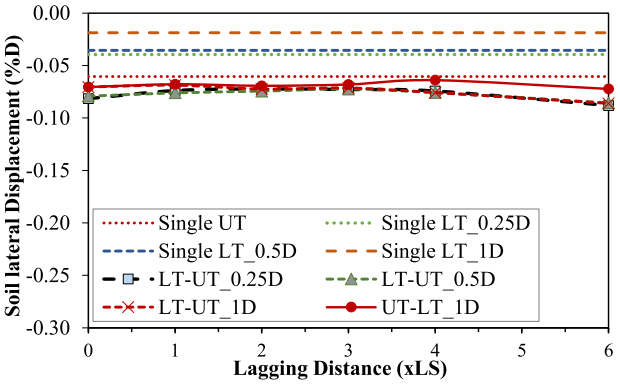

Fig. 16. Soil's maximum lateral displacements along the TS axis of the single tunnel and twin stacked tunnels depending on L_F.

movements (from 114 to 120%) are observed when the upper-lower tunnel excavation sequence is applied (i.e., scenarios 4, 5, and 6) (Table 5). Table 5 also presents the influence of the twin stacked tunneling sequence on the maximum lateral soil movement. It decreases when the pillar depth between tunnels increases from 0.25D to 1D, represented by X_{LU}/X_{UL} ratio changed, respectively, from 127.94 to 119.16%.

It is interesting to note from the soil displacements profiles in Fig. 14 that after completing the twin stacked tunnel excavation, lateral inward soil movements at the spring line of each tunnel increase slightly in comparison with the single tunnel case at the same depth when this tunnel is excavated first. In other words, when the upper tunnel is excavated after the lower tunnel, inward lateral soil movements at the upper tunnel's spring line are greater than in the case where the upper tunnel is excavated first. The reason could be related to (1) the stress release taking place in the soil (Soomro et al., 2021b), (2) the discrepancy decrease of vertical and lateral stresses in the soil zone surrounding the following tunnel disturbed by the first tunneling construction (Do et al., 2014a). It causes a decrease in oval deformation of the tunnel lining and therefore in the soil's lateral outward movement at the tunnel side. The above findings help to demonstrate that for scenarios 1, 2, and 3, where the upper tunnel is excavated above the existing lower tunnel, the inward lateral soil movements are induced to a greater extent than in scenarios 4, 5, 6, respectively, in which the upper tunnel is excavated first. This result is supported by the larger maximum settlement and steeper settlement observed in scenarios 4, 5, and 6 when compared with scenarios 1, 2, and 3 (Fig. 5).

With respect to the lagging distance effect, Fig. 16 illustrates the different influences of lagging distance on the maximum lateral soil movements depending on the tunnels pillar depth. When the pillar depth is smaller than 0.5D, i.e., scenarios 1 and 2, the smallest inward lateral soil movements are observed at a lagging distance of 3D. Nevertheless, for greater pillar depths (1D), the larger the lagging distance is, the

higher the maximum inward lateral soil movements are, regardless of the construction sequence. It should be mentioned that the lateral soil movement variation depending on the lagging distance is negligible.

3.3. Lining displacements in the tunnel lining

In this section, Figs. 17 and 18 present the normal displacement profiles in the upper and lower tunnels, respectively, considering different tunneling procedure scenarios. It is noted that positive and negative normal displacements correspond to inward and outward displacements of the tunnel lining. Figs. 19 and 20 show the maximum inward and outward displacements developed in the upper and lower tunnels. Normal displacements presented in Figs. 17 to 20 were determined in cases where the following tunnel is excavated when the preceding tunnel reached a steady-state, i.e., $L_F = 6L_S$.

It can be seen from Fig. 17 that the displacements induced in the upper tunnel are strongly affected by the tunneling sequence but not by the tunnels pillar depth. When the upper tunnel is excavated above the existing lower tunnel, displacements in the following upper tunnel are similar to the single upper ones regardless of the tunnels pillar depth. However, when the upper tunnel is excavated first and followed by the lower tunnel, great increases of the inward displacements at the crown and outward displacements at the bottom of the upper tunnel are observed (Fig. 17). This is due to the soil settlements induced in the pillar zone between tunnels during the lower tunneling as seen in Fig. 11 and observed by Do et al. (2014a), Islam and Iskander (2021). The same finding was obtained by Addenbrooke and Potts (2001) who stated that the distortion and displacement of the existing lining are greater if the second tunnel passes beneath rather than above the existing tunnel. It is

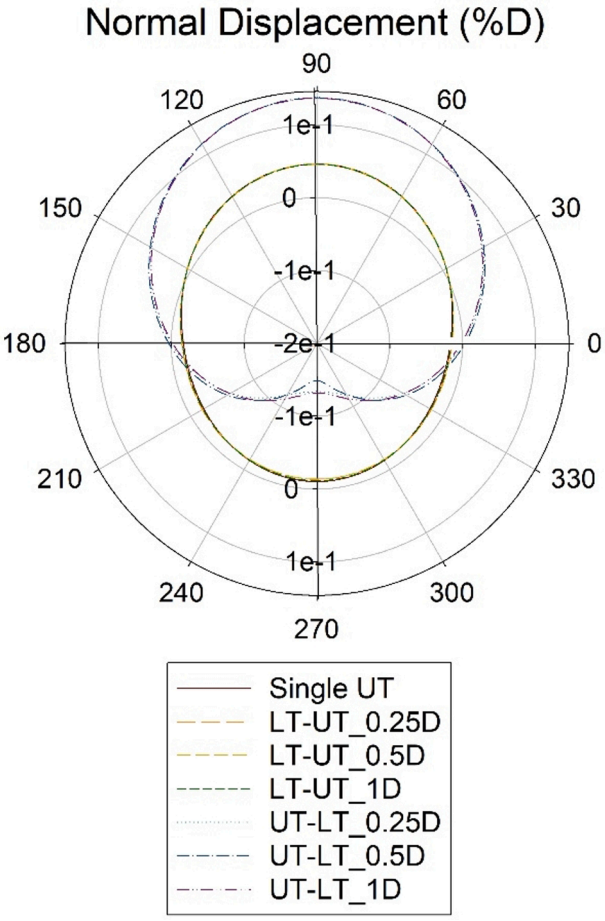

Fig. 17. Normal displacement induced in the upper tunnel ($L_F = 6L_S$).

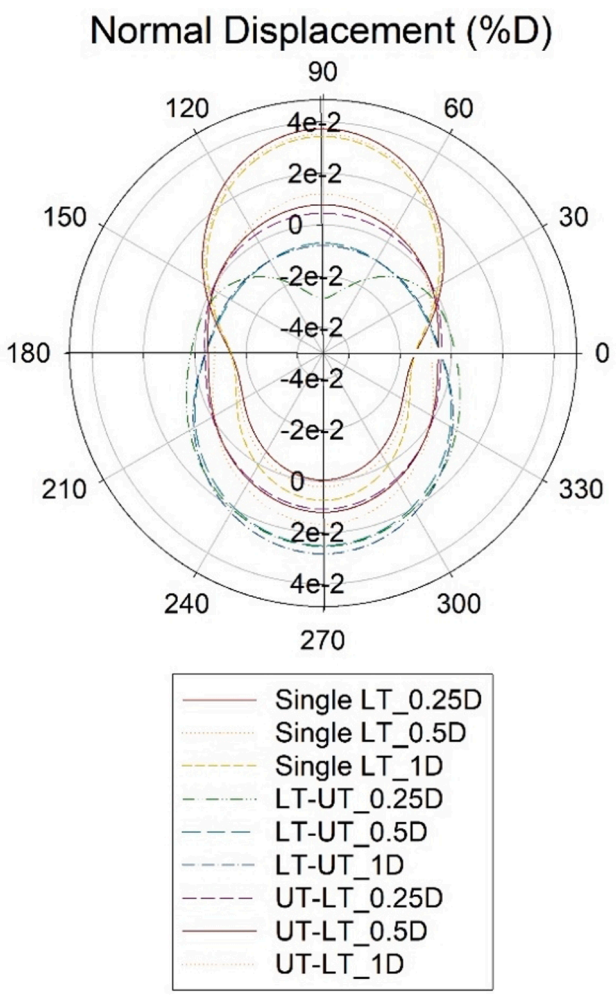

Fig. 18. Normal displacement induced in the lower tunnel ($L_F = 6L_S$).

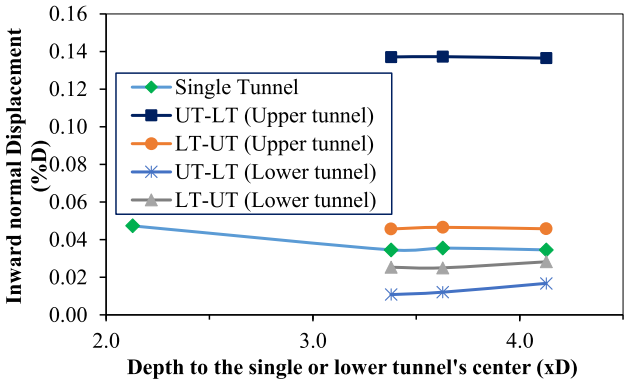

Fig. 19. Maximum inward displacement induced in the tunnels ($L_F = 6L_S$).

interesting to note that the maximum incremental inward movements at the upper tunnel crown (0.08 %D) are smaller than the maximum incremental outward movements at the upper tunnel bottom (0.12 %D-0.138 %D) (subtraction of corresponding lines in Figs. 19 and 20). It means that the lining to the existing upper tunnel elongates in the vertical direction, giving an increase in the vertical diameter and a reduction in the horizontal diameter. The same observation was obtained by Yamaguchi et al. (1998) and Addenbrooke and Potts (2001).

Unlike for the upper tunnel, displacements in the lower tunnel lining are considerably influenced by both tunneling sequences and pillar

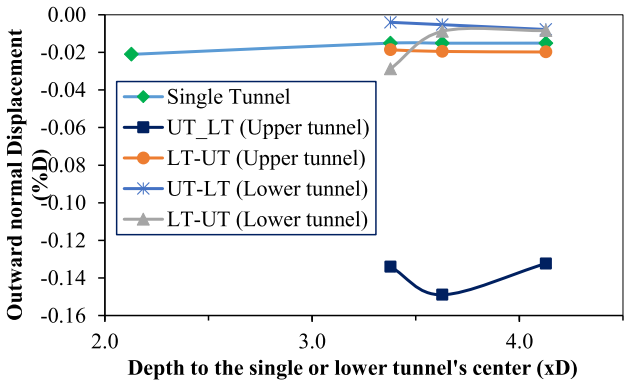

Fig. 20. Minimum outward displacement induced in the tunnels ($L_F = 6L_S$).

depth (B) (Fig. 18). The lower–upper tunneling sequences (i.e., scenarios 1, 2, and 3) caused a stronger effect than those of the upper-lower tunneling procedures. When the lower tunnel is excavated below the existing upper tunnel, inward displacements at the lower tunnel's crown decrease compared with the single lower tunnel ones. The reason is firstly due to the reinforcement effect of the upper tunnel (Li and Yuan, 2012; Islam and Iskander, 2021) which works as a barrier and helps to reduce the strata impact on the lower tunnel. Secondly, the soil at the upper tunnel's bottom is upheaved and strained before the excavation of the lower tunnel, thus downward movement at the lower tunnels' crown decreases. A reduction of approximately 90,02%, 83,11% and 73.72% corresponding to the pillar depth (B) of 0.25D, 0.5D and 1D is observed. It means that the higher the pillar depth between tunnels, the lower the influence of the existing upper tunnel on the inward displacements at the crown of the lower tunnel. When the lower tunnel is excavated first, the following excavation of the upper tunnel causes uplift movement in the existing lower tunnel as indicated in Fig. 17 and observed by Addenbrooke and Potts (2001), Do et al. (2014a), Islam and Iskander (2021). Consequently, the lower tunnel crown is upwardly deformed as can be seen in Fig. 18. An increase of the pillar depth between tunnels leads to a decrease of the upheaval impact caused by the upper tunnel and therefore upward movements of the lower tunnel. Thus, the largest upheaval displacements at the lower tunnel's crown are observed in the case of a pillar depth (B) of 0.25D (Fig. 18 and Fig. 20).

Concerning the displacements at the bottom of the lower tunnel, twin stacked tunnels always produce inward displacements due to the uplift effect caused by the following upper tunnel construction (scenarios 4, 5, and 6) or a reinforcement beam action of the existing upper tunnel (scenarios 1, 2 and 3) as mentioned earlier. The larger inward displacements at the lower tunnel's bottom are seen when the upper tunnel is excavated above the existing lower tunnel (scenarios 1, 2, and 3).

After finishing both twin stacked tunnels construction, Figs. 19 and 20 indicate that the greatest inward and outward displacements occur, respectively, in the crown and bottom of the upper tunnel caused by the settlement effect due to the following lower tunnel construction. This scenario also leads to the smallest inward and outward displacements in the lower tunnel compared with those of a single tunnel. In other words, scenarios where the lower tunnel is excavated first often produce smaller variations in the lining displacements for both the upper and lower tunnels.

With respect to the lagging distance between tunnel faces considering the tunnels pillar depth change, Figs. 21 and 22 illustrate the considerable influence of lagging distance on tunnel linings displacements. When the lower tunnel is constructed first then followed by the upper tunnel (scenarios 1, 2, and 3), pillar depth (B) has a negligible impact on the relationship between the upper tunnel lining displacements and lagging distances (Fig. 21). In other words, at a certain lagging distance (L_F), extreme inward and outward displacements in the upper tunnel are nearly similar for any of the considered pillar depths

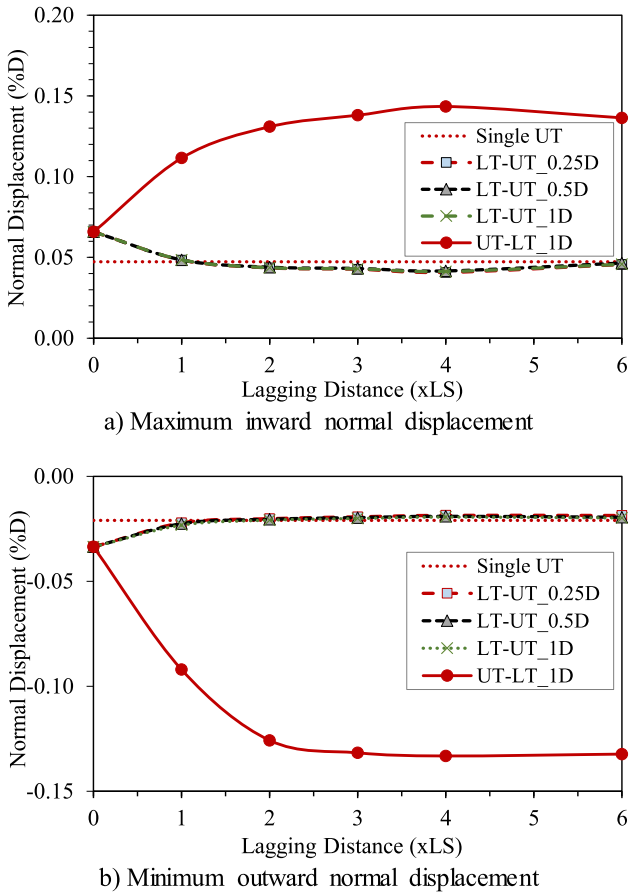

Fig. 21. Normal displacement induced in the upper tunnel lining depending on the lagging distance L_F.

(B) of 0.25D, 0.5D, and 1D. The same observation for the inward displacements in the lower tunnel is presented in Fig. 22a. However, outward displacements induced in the lower tunnel caused by the excavation of the following upper tunnel are strongly influenced by the pillar depth (B) between tunnels, and in particular by the lagging distance (Fig. 22b).

For the upper tunnel, the greatest extreme lining displacements in scenarios 1, 2, and 3 are observed when two stacked tunnels are excavated concurrently, i.e., $L_F = 0$ (Fig. 21). There is then a considerable decrease in the extreme lining displacement for a lagging distance of $1L_S$. A continued increase of the lagging distance after that is followed by a slight decrease of the extreme displacement in the upper tunnel when compared to the single upper tunnel case (Fig. 21). The reason is related to the oval displacement of the tunnel lining with a small lateral earth pressure coefficient ($K_0 = 0.5$) which implies inward movements at the crown and bottom, and an outward movement at the two sides of the single tunnel. An increase of the lagging distance induces a longer redistribution process of the stress–strain in the soil above the excavated lower tunnel before the following upper tunnel face passes through. It means that the following upper tunnel is excavated in a more deformed soil mass and more uniform soil stresses. It, therefore, causes smaller displacements in the upper tunnel lining. Unlike scenarios 1, 2, and 3, in scenario 6 where the following lower tunnel is constructed underneath the preceding upper tunnel with a 1D pillar depth, a lagging distance increase between the tunnels is followed by great increments of the inward displacements and outward displacements at the crown and base, respectively, of the upper tunnel (Fig. 21). This is due to the supplementary settlement of the upper tunnel caused by the excavation of the following lower tunnel as indicated in Fig. 11 and mentioned earlier by Islam and Iskander (2021). A longer lagging distance between the tunnel

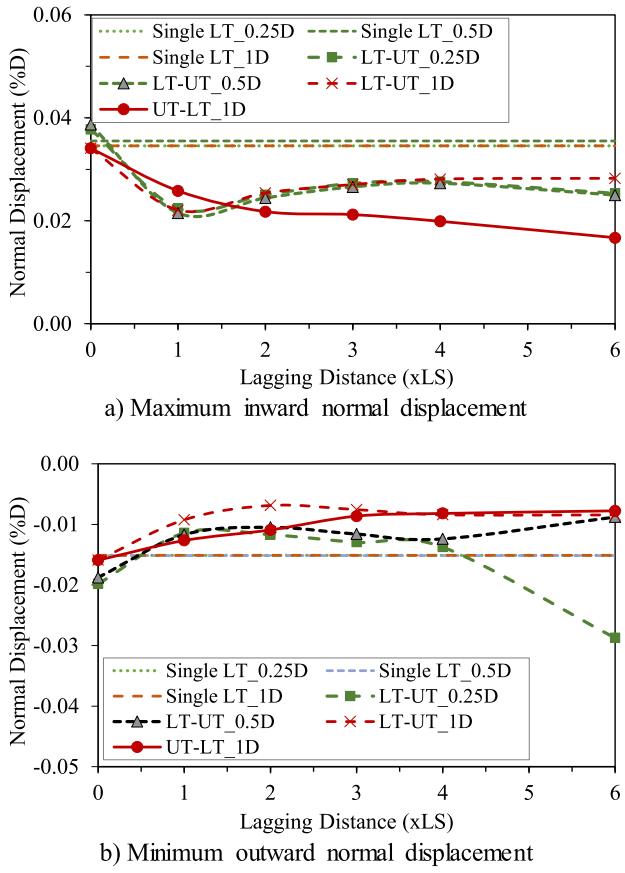

Fig. 22. Normal displacement induced in the lower tunnel lining depending on the lagging distance L_F.

faces allows more complete soil settlement above the following lower tunnel and therefore a higher amount of outward and inward displacements at the bottom and crown, respectively, of the preceding upper tunnel. The above results support the conclusion that the upper-lower tunnel construction sequence causes a strongly adverse behavior to the upper tunnel.

Compared to Fig. 21, Fig. 22 indicates that at the largest lagging distance of the twin stacked tunnels, regardless of the tunnel construction sequence, displacements in the lower tunnel are much smaller than in the upper tunnel, in particular for the inward displacements at the tunnel's crown. The smallest inward displacements induced at the crown of the lower tunnel in scenarios 1, 2, and 3 are seen at a lagging distance $L_F = 1L_S$ (Fig. 22a). This means the upper tunnel face is at the same cross-section as the lower tunnel shield tail. This situation results in the fact that downward displacements of the lower tunnel crown have not completely developed yet before the upper tunnel passes through and thus cause the uplift effect on the lower tunnel. Clearly, a greater lagging distance allows a larger downward displacement at the lower tunnel crown under the impact of ground pressure. When the lower tunnel is excavated underneath a preceding upper tunnel (scenario 6), downward displacements at the lower tunnel crown (Fig. 22a) decrease when the lagging distance increases large enough. The reason is related to the completeness of the upward movements at the preceding upper tunnel bottom due to the low lateral earth pressure effect before the passage of the following lower tunnel (Fig. 13). As a result, downward movements occur above the lower tunnel excavated later, and therefore inward displacements at the lower tunnel's crown are reduced with the lagging distance increase (Fig. 22a).

Fig. 22b indicates a slight influence of the lagging distance on the outward displacements mostly on the lower tunnel sides, except for the situation when $L_F = 6L_S$ in scenario 1 (small pillar depth of 0.25D) is considered. In these circumstances, outward displacements are seen at the lower tunnel crown. They are strongly affected by the uplift effect during the following upper tunnel construction. It is clearer when looking at Fig. 23 which presents the distribution of the normal displacement along with the lower tunnel boundary in scenario 1 for a pillar depth (B) of 0.25D. As indicated in Fig. 12, for a short lagging distance (L_F), the effect of the uplift behavior is less important and therefore leads to a decrease in the upward movements of the lower tunnel crown (Fig. 23). When the lagging distance is large enough, which corresponds to the situation where the upper tunnel is excavated after finishing the lower tunnel, the greatest upward displacements are seen at the lower tunnel's crown. Fig. 23 also indicated that at the most lagging distance, an inward displacement increment of the lining at the lower tunnel's bottom relating to the uplift effect is predicted.

For larger tunnels pillar depth (B), the uplift effect caused by the following upper tunnel that takes place in the preceding lower tunnel decreases. Thus, the results in Fig. 22b did not show a great decrease in the inward displacements at the lower tunnel's crown.

3.4. Normal forces and longitudinal forces in the tunnel lining

Fig. 24 and Table 6 present the maximum normal forces in a single tunnel and twin tunnels in the circumstances where the following tunnel is constructed after the preceding tunnel, i.e., $L_F = 6L_S$, without considering the lagging distance effect. Figs. 25 and 26 show the effect of the lagging distance between tunnel faces and tunnels pillar depth on the normal forces induced in both tunnels. It can be seen from Fig. 26 and Table 6 that normal forces in the deeper single tunnel are always greater than the ones in the shallower tunnel. They are caused by the gravity

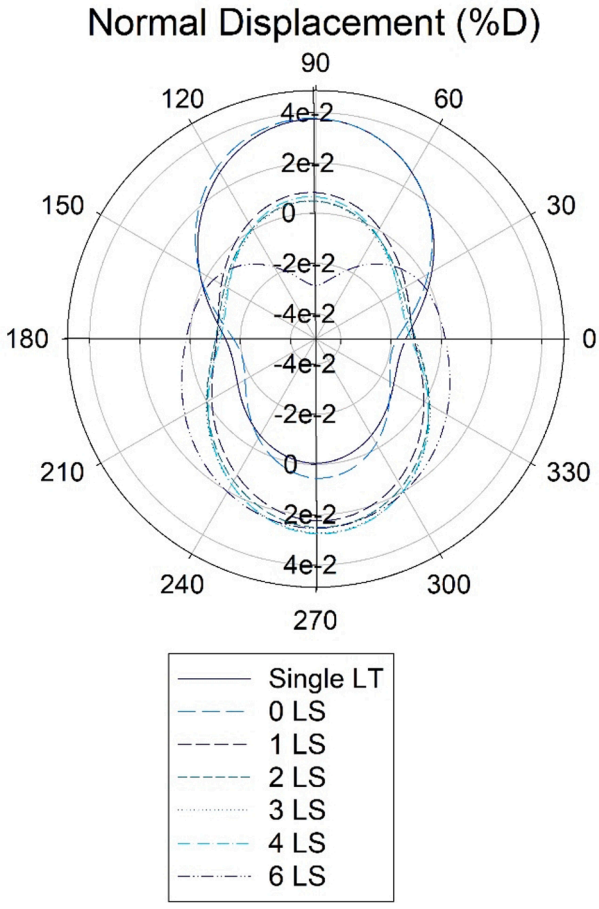

Fig. 23. Normal distribution along with the lower tunnel boundary in Scenario 1.

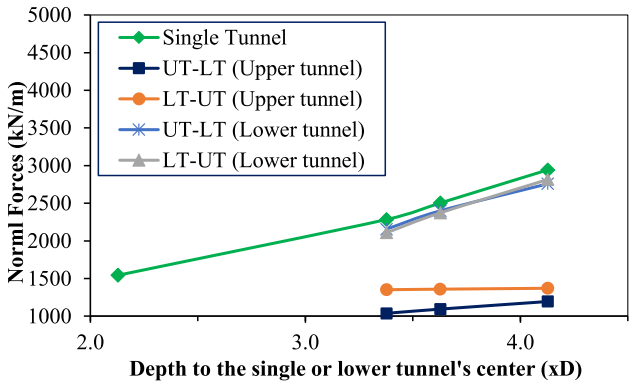

Fig. 24. Maximum normal forces induced in the single tunnel and twin stacked tunnels ($L_F = 6L_S$).

Table 6
Maximum normal forces in single and twin stacked tunnels ($L_F = 6L_S$).

Scenarios	1 or 4	2 or 5	3 or 6
Depth to the lower tunnel's center (D)	3.4	3.6	4.1
	Maximum normal force (kN/m)		
Single LT (N_L)	2284	2503	2942
Single UT (N_U)	1545		
Normal forces in the upper tunnel			
Scenarios 1, 2, 3: NU_{LU}	1352	1359	1370
Scenarios 4, 5, 6: NU_{UL}	1037	1094	1196
NU_{LU}/N_U (%)	87.5	88.0	88.7
NU_{UL}/N_U (%)	67.1	70.8	77.4
NU_{LU}/NU_{UL} (%)	130.3	124.2	114.6
Normal forces in the lower tunnel			
Scenarios 1, 2, 3: NL_{LU}	2110	2373	2816
Scenarios 4, 5, 6: NL_{UL}	2156	2399	2874
NL_{LU}/N_L (%)	92.4	94.8	95.7
NL_{UL}/N_L (%)	94.4	95.8	97.7
NL_{LU}/NL_{UL} (%)	97.8	98.9	98.0
The ratio of normal forces in upper and lower tunnels (%)			
Scenarios 1, 2, 3: NU_{LU}/NL_{LU}	64.1	57.3	48.7
Scenarios 4, 5, 6: NU_{UL}/NL_{UL}	48.1	45.6	41.6

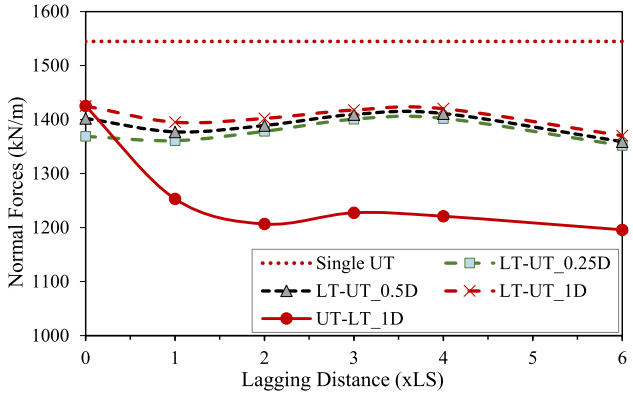

Fig. 25. Maximum normal forces induced in the upper tunnel lining.

stresses increasing with depth. In addition, the excavation of twin stacked tunnels causes a decrease in the normal forces induced in the lining for both tunnels compared to the observed ones in a single tunnel.

Concerning the upper-lower tunneling sequence (scenarios 4, 5, and 6), Fig. 24 and Table 6 show that normal forces in the upper tunnel are smaller. Ratios NU_{UL}/N_U are varied in a range from 67.1 to 77.4% when the pillar depth (B) changes from 0.25D to 1D, respectively. Meanwhile, normal forces in the lower tunnel are less influenced by the upper

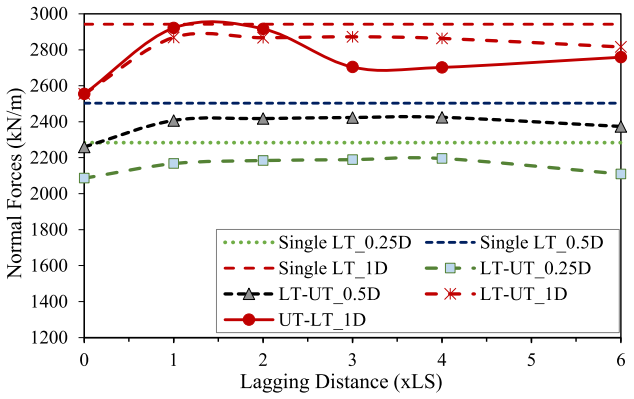

Fig. 26. Maximum normal forces induced in the lower tunnel lining.

existing tunnel, and the ratio NL_{UL}/N_L varied from 94.4 to 97.7%. The normal forces decrease in the upper tunnel resulting from the following lower tunnel construction could be explained by the settlement effect induced in the upper tunnel. The downward soil movements towards the lower tunnel, caused by the convergence displacement along the lower tunnel, can be considered as the reason for the reduction of the normal forces in the bottom region of the upper tunnel. Insignificant changes in the normal forces at the crown part of the upper tunnel are observed. The zones between the two stacked tunnels are principally influenced by the twin tunneling interaction. This is likewise why a larger distance (B) between tunnels caused a smaller discrepancy between normal forces in twin stacked tunnels and the corresponding single tunnel as indicated above.

When the lower tunnel is excavated first (scenarios 1, 2, and 3), normal forces induced in the second upper tunnel are smaller than that of the single upper tunnel case and insignificantly influenced by the pillar depth between tunnels (Fig. 24). The reason could be concerned with the soil stiffness reduction above the lower tunnel in which the upper tunnel is then excavated. The ratio NU_{LU}/N_U is more or less constant and stays in the range of 87.5 to 88.7%. Values varying between 130.3 and 114.6% are higher than those in scenarios 4, 5, and 6 when the upper tunnel is excavated first. The normal forces change of the lower tunnel represented by the ratio NL_{LU}/N_L is smaller than for the upper tunnel and varied from 92.4 to 95.7% (Fig. 24 and Table 6).

The above results support the following conclusions: Firstly, twin stacked tunneling sequences have a more important impact on the normal forces in the upper tunnel but less on the lower tunnel; Secondly, the influence of the twin stacked tunnels construction procedure decreases for high tunnels pillar depth (B). The ratio between normal forces in the upper and lower tunnels of NU_{LU}/NL_{LU} (in scenarios 1, 2, and 3) and NU_{UL}/NL_{UL} (in scenarios 4, 5, and 6) is lower when the pillar depth (B) increases. It is also interesting to show that when the lower tunnel is excavated first, the ratio between normal forces in the upper and lower tunnels of (NU_{LU}/NL_{LU}) is always larger than the corresponding one in cases of upper tunnel excavating first (NU_{UL}/NL_{UL}) (Table 6).

Fig. 25 presents a noticeable influence of the lagging distance on the normal forces in the upper tunnel for both construction sequences. When the upper tunnel is excavated above the existing lower tunnel (scenarios 1, 2, and 3), high normal forces are observed at the lagging distance L_F of 0. They are then followed by a significant decrease when the lagging distance increase to 1 L_S. A continued increase in lagging distance causes a rise in the normal forces. However, when the lagging distance is large enough, i.e., the upper tunnel is excavated when the lower tunnel reached a steady-state ($L_F = 6L_S$), a normal forces reduction is observed. The normal forces decrease at the lagging distance $L_F = 1L_S$ could be explained by the downward soil movements taking place below the upper tunnel bottom and above the lower tunnel. The reason is due to the convergence displacements along with the lower tunnel's shield.

These downward movements caused a pressure decrease acting from the surrounding soil on the bottom of the upper tunnel lining and thus a decrease in normal forces. At a larger lagging distance, the uplift effect induced in the lower tunnel caused by the following upper tunnel as indicated in Fig. 12 and by Islam and Iskander (2021) plays a more important role and results in a recovery of vertical movements toward the upper tunnel. It, therefore, leads to a soil pressure increase applied on the upper tunnel bottom. Nevertheless, for a very high lagging distance, where the maximum soil downward movements above the lower tunnel are reached at the steady-state, a soil pressure decrease acting on the upper tunnel bottom is predicted. It causes a reduction of the normal forces in the upper tunnel lining as mentioned above. In Fig. 25, the lagging distance influence the normal forces in the upper tunnel in scenarios 1, 2, and 3 has the same tendency.

In scenario 6 where the upper tunnel is excavated first and followed by the lower tunnel at a pillar depth (B) of 1D, a lagging distance increase is followed by a larger decrease of the normal forces in the upper tunnel (Fig. 25). The reason can be due to the supplementary settlement effect induced in the upper tunnel caused by the following lower tunnel as described in Fig. 13 and also by Addenbrooke and Potts (2001), Islam and Iskander (2021). The greater lagging distance between tunnels induces a longer influencing range in the longitudinal direction from the lower tunnel to the upper tunnel. Consequently, larger downward soil movements above the lower tunnel are observed, and thus a reduction of the normal forces in the upper tunnel could be anticipated.

Unlike for the upper tunnel, normal forces in the lower tunnel are slightly affected by the lagging distance between stacked tunnels in scenarios 1, 2, and 3, except when tunnels are excavated concurrently (Fig. 26). For most of the lagging distances, twin stacked tunnels cause slight normal forces to decrease in the lower tunnel compared with a single tunnel constructed at the corresponding depth. They can be represented by ratios NL_{LU}/N_L and NL_{UL}/N_L of 92.4 to 97.7% (Table 6). In scenario 6, when the upper tunnel is excavated first, the smallest normal forces induced in the lower tunnel are seen when two tunnels are excavated concurrently (Fig. 26). The largest normal forces occurred at the lagging distance $L_F = 1 - 2L_S$, and then decrease when the lagging distance increased. The reason is related to the upward soil movements induced at the preceding upper tunnel bottom. Indeed, as mentioned in section 3.3 (Fig. 13), due to the low lateral earth pressure coefficient effect, upward movements at the upper tunnel base are much more taken place before the passage of the following lower tunnel when the lagging distance increases. It causes a reduction of the downward soil movements and therefore of the pressure applied on the lower tunnel crown. Consequently, the normal forces in the lower tunnel decrease with the lagging distance increase from $2L_S$ to $4L_S$ as illustrated in Fig. 26. This result is also consistent with the decrease of the inward displacements at the lower tunnel crown indicated in Fig. 22a.

Figs. 27 and 28 highlight the lagging distance impact on the longitudinal forces in the tunnel lining. The maximum longitudinal forces in the preceding tunnel are obtained when the face of the following tunnel is at the same cross-section as the shield tail of the preceding tunnel. The jacking forces effect at the shield tail of the preceding tunnel and support pressure applied at the following tunnel face are the main reasons for the sudden increase of the longitudinal forces induced in the preceding tunnel as can be seen in Fig. 27 for the upper tunnel and in Fig. 28 for the lower tunnel. In addition, cylindrical pressures that act in the working chamber of the following tunnel can also cause a load transfer from this tunnel toward the preceding tunnel. An increase in the external loads in the radial direction and followed by an increase in the longitudinal forces in the lining of the preceding tunnel due to the Poisson effect can therefore be predicted (Do et al., 2014a; Do et al., 2016). It is noticeable that the above relationship is reproduced for all tunnel construction sequence scenarios.

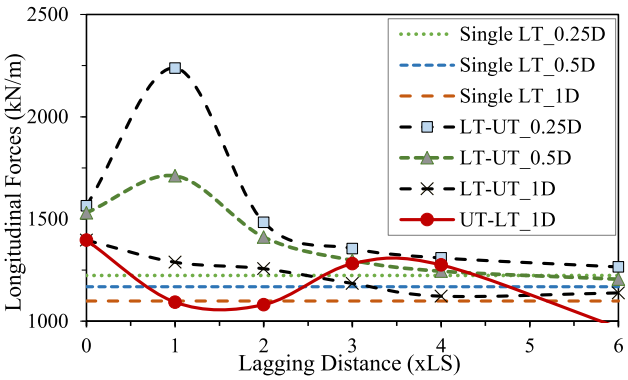

Fig. 28. Maximum longitudinal forces induced in the lower tunnel lining.

At the lagging distance of $2L_S$, a strong decrease of the longitudinal forces of the preceding tunnel is seen. When the following tunnel is excavated further behind the preceding tunnel, i.e., $L_F > 2L_S$, a slight decrease of the longitudinal forces is observed. Unlike for the preceding tunnel, the greater lagging distance between tunnels results in slightly longitudinal forces decrease in the following tunnel (Figs. 27 and 28).

3.5. Bending moments in the tunnel lining

Fig. 29 and Table 7 present the maximum bending moment in single or twin tunnels in situations where the following tunnel is constructed after the preceding tunnel, i.e., $L_F = 6L_S$ without considering the lagging distance effect. Due to the low lateral earth pressure coefficient value, laterally ovalling displacements of the tunnel lining are predicted for a single tunnel. It means that while positive bending moments are observed at the crown and bottom, negative values are seen at the tunnel sides.

Fig. 29 and Table 7 show that bending moments in the lower tunnel

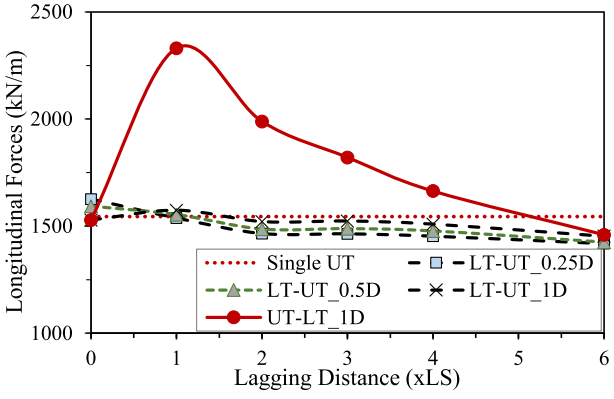

Fig. 27. Maximum longitudinal forces induced in the upper tunnel lining.

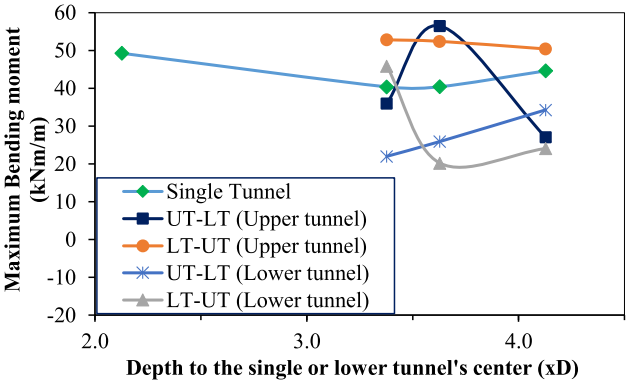

Fig. 29. Maximum bending moment induced in the single tunnel and twin stacked tunnels ($L_F = 6L_S$).

Table 7
Maximum bending moment in the single tunnel and twin stacked tunnels ($L_F = 6L_S$).

Scenarios	1 or 4	2 or 5	3 or 6
Depth to the lower tunnel's center (D)	3.4	3.6	4.1
	Maximum bending moment (kN.m/m)		
Single LT (M_L)	40.4	40.4	44.6
Single UT (M_U)	49.3		
Bending moment in the upper tunnel			
Scenarios 1, 2, 3: MU_{LU}	52.8	52.4	50.4
Scenarios 4, 5, 6: MU_{UL}	36.0	56.5	27.0
MU_{LU}/M_U (%)	107.2	106.3	102.3
MU_{UL}/M_U (%)	73.0	114.6	54.9
MU_{LU}/MU_{UL} (%)	146.7	92.8	186.4
Bending moment in the lower tunnel			
Scenarios 1, 2, 3: ML_{LU}	45.9	20.2	24.1
Scenarios 4, 5, 6: ML_{UL}	22.0	25.9	34.3
ML_{LU}/M_L (%)	113.6	50.0	53.9
ML_{UL}/M_L (%)	54.5	64.0	76.8
ML_{LU}/ML_{UL} (%)	208.6	78.0	70.2
The ratio of bending moment in upper and lower tunnels (%)			
Scenarios 1, 2, 3: MU_{LU}/ML_{LU}	115.1	259.3	209.4
Scenarios 4, 5, 6: MU_{UL}/ML_{UL}	163.6	218.1	78.9

are usually lower than those in the upper tunnel. Indeed, ratios MU_{LU}/ML_{LU} and MU_{UL}/ML_{UL} are larger than 100%, except in scenario 6 (Table 7). This implies that the discrepancy between vertical and lateral external loadings surrounding the lower tunnel is smaller than those applied in the upper tunnel. This conclusion is consistent with the small displacements induced in the lower tunnel mentioned in section 3.3. To clarify the irregular bending moments change for some scenarios as seen in Fig. 29, the bending moment distribution along the upper tunnel boundary in scenarios 4, 5, 6, and of the lower tunnel in scenarios 1, 2, and 3 are presented in Figs. 30 and 31, respectively.

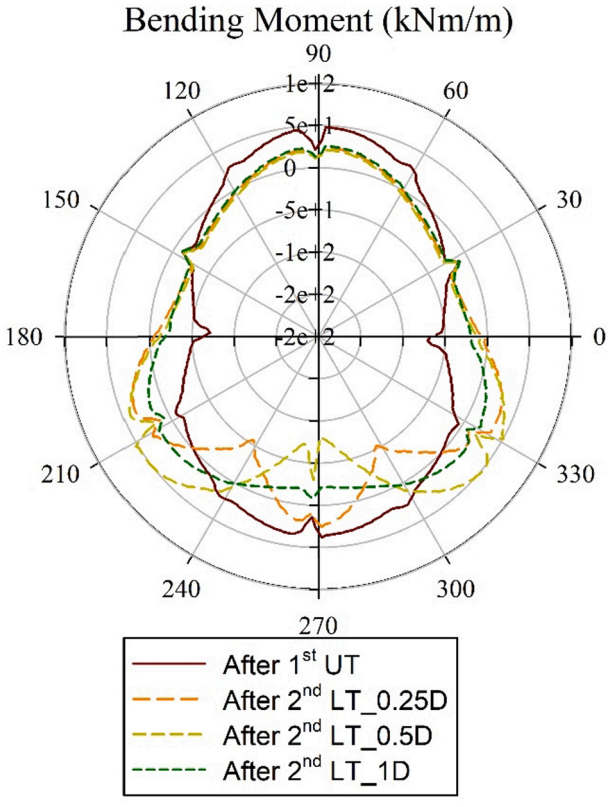

Fig. 30. Bending moment distribution in the upper tunnel in scenarios 4, 5, 6 ($L_F = 6L_S$).

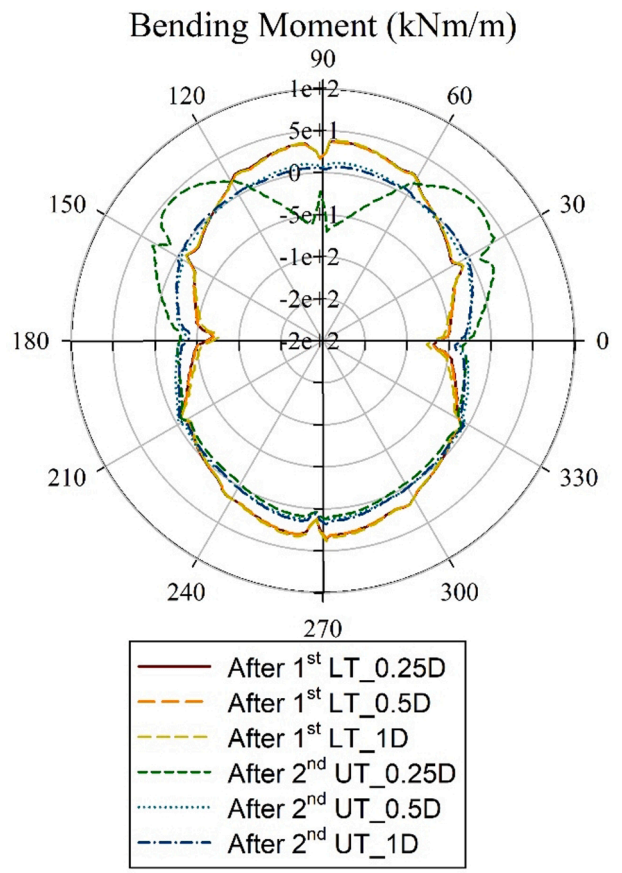

Fig. 31. Bending moment distribution in the lower tunnel in scenarios 1, 2, 3 ($L_F = 6L_S$).

As mentioned in section 3.1, the excavation of the lower tunnel below the existing upper tunnel causes a downward soil movement between tunnels. Hence, the upper tunnel tends to settle. It causes a reduction of the positive bending moment at the upper tunnel crown as seen in Fig. 30. Meanwhile, greater downward movements are predicted in the bottom area of the upper tunnel. At the pillar depth (B) of 0.25D, due to the small pillar depth, the downward movement originated from the convergence along the lower shield is partly offset by the action of forces applied in the lower shield, such as grouting and cylindrical pressure. A slight change in the bending moment at the tunnel base is therefore observed. When increasing the pillar depth between tunnels, B = 0.5D, the action of forces from the lower tunnel shield is reduced allowing a greater downward soil movement in the pillar zone. It helps to explain the outward displacements at the bottom of the upper tunnel lining leading to a stronger change from positive to negative bending moment values as seen in Fig. 30. At the higher pillar depth of 1D, the impact of the lower shield becomes negligible. It is also followed by a reduction of the downward movements in the pillar zone due to the tunnel interaction decrease and therefore causes a smaller change in the bending moments in comparison with the case of B = 0.5D mentioned above.

In contrast to the upper tunnel in which the bending moments variation is mainly seen at the tunnel base, an important bending moment change in the lower tunnel occurs at the tunnel crown when the upper tunnel is excavated followingly (Fig. 31). The main reason is due to the uplift effect induced in the lower tunnel caused by the upper tunnel excavation mentioned earlier. It can, therefore, be seen from Fig. 31, that at a small pillar thickness (B) of 0.25D, the bending moment at the lower tunnel's crown changes greatly from positive to negative values. For larger pillar thicknesses of 0.5D and 1D, a lighter uplift effect

caused by the upper tunnel is predicted. It leads to a smaller alteration of the bending moments at the lower tunnel's crown. In all the cases, the excavation of the following upper tunnel causes a slight upheaval at the lower tunnel lining base resulting in a decrease of the positive bending moment.

Figs. 32 and 33 show the effect of the lagging distance between tunnel faces and pillar depth between tunnels on the bending moments induced in both twin tunnels. Fig. 32 illustrates a marked influence of the lagging distance on the bending moment in the upper tunnel for both construction sequences, i.e., lower–upper tunnels and upper-lower tunnels. When the upper tunnel is excavated above the existing lower tunnel (scenarios 1, 2, and 3), the smallest maximum bending moment in the upper tunnel (obtained at its crown) is generally observed at a lagging distance L_F of about $3L_S$ (Fig. 32). It is probably due to the deformed soil zone above the lower preceding tunnel excavation. For shorter lagging distances, i.e., L_F of about 1 to $2L_S$, the deformed quantity of soil above the lower tunnel is still rising and, therefore, causes a larger pressure applied in the upward direction on the upper tunnel lining which is passing through. Consequently, higher positive bending moments are seen when L_F is equalling 1 to $2L_S$. However, at a longer lagging distance, the increase of the bending moment at the upper tunnel lining's crown, (102.3 to 107.2%) is larger than in the single tunnel case (Table 7 and Fig. 32). This is probably due to the complete uplift effect of the lower tunnel which causes a slight upward movement above the lower tunnel and hence the upper tunnel. A slight decrease in the surface settlements observed in the numerical result (case $L_F = 6L_S$) compared with the $L_F = 3L_S$ case demonstrates this phenomenon.

Unlike scenarios 1, 2, and 3, in scenario 6 where the upper tunnel is excavated first and followed by the lower tunnel at a pillar depth (B) of 1D, Fig. 32 indicates a decrease in the maximum bending moment induced at the upper tunnel crown when the lagging distance L_F increase. The settlement effect induced in the upper tunnel caused by the following lower tunnel helps to explain this relationship. Indeed, a longer lagging distance means a larger downward movement below the upper tunnel and therefore the whole upper lining when the lower tunnel passes through followingly. It causes a vertical pressure decrease applied on the top of the upper tunnel and, consequently, leads to a smaller positive bending moment at the upper tunnel's crown.

Fig. 33 presents a slightly decreased tendency of the maximum bending moments in the lower tunnel when increasing the lagging distance between the preceding lower tunnel and the following upper tunnel (scenarios 1, 2, and 3). In addition, scenario 6 where the upper tunnel is excavated first commonly leads to a smaller maximum bending moment in the lower tunnel compared to the corresponding single lower tunnel, except for very short lagging distances. The reason is related to the reinforcement effect of the upper tunnel formed above the top of the lower tunnel which helps to decrease the vertical pressure applied on the lower tunnel's crown and therefore the bending moments. This also allows explaining the greatest maximum bending moments in the lower tunnel when twin stacked tunnels are excavated concurrently (see Fig. 33) because of the missing reinforcement effect of the upper tunnel in this situation.

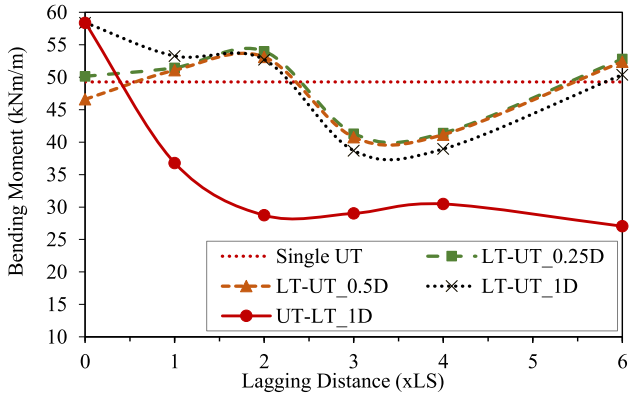

Fig. 32. Maximum bending moment induced in the lining of the upper tunnel.

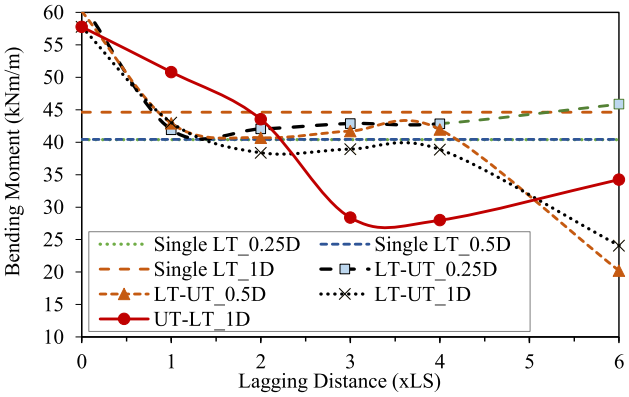

Fig. 33. Maximum bending moment induced in the lining of the lower tunnel.

4. Conclusion

A numerical investigation of twin stacked mechanized tunneling is performed to highlight (1) the lagging distance effect between two tunnels' faces, (2) the tunnels pillar depth, and (3) the tunneling excavation sequences on the soil movements, structural forces, and deformations induced in the lining for both tunnels. The following comments can be drawn based on the results obtained in the present study:

- The construction sequence, pillar depth, and lagging distance of twin stacked tunnels cause a considerable influence on the soil movements and behavior of the tunnel lining;
- During twin stacked tunnels construction, while the maximum settlement is strongly dependent on the upper tunnel, the width of the settlement is more affected by the lower tunnel. The lagging distance between two stacked tunnel faces and pillar depth have an insignificant influence on the settlement at the ground surface. The excavation sequences have an important influence on the settlement trough. The adverse situation is when the upper tunnel is excavated first;
- The excavation of twin stacked tunnels leads to an increase in the lateral soil movements at both tunnels' spring lines and the lagging distance has a negligible influence on the lateral soil movements;
- Normal displacements induced in the upper tunnel are strongly affected by the tunneling sequence but not by the tunnels pillar depth (B). However, unlike for the upper tunnel, displacements in the lower tunnel lining are influenced by both tunneling sequences and pillar depth (B). For most of the lagging distances of twin stacked tunnels, regardless of the tunnel construction sequence, displacements in the lower tunnel are greatly smaller than in the upper tunnel;
- Twin stacked tunneling sequences have a more significant impact on the normal forces in the upper tunnel than in the case of the lower tunnel. Moreover, the construction procedure influence of twin stacked tunnels decreases for higher tunnels pillar depth (B). Lagging distance has a noticeable influence on the normal forces in the upper tunnel in both construction sequences but not on the tunnels pillar depth. However, the normal forces in the lower tunnel are slightly affected by the lagging distance between stacked tunnels in scenarios 1, 2, and 3 but not in scenario 6;
- Bending moments in the lower tunnel are lower than in the upper tunnel. Variations of the bending moments in the upper tunnel are mainly located at the tunnel base and at the tunnel crown for the lower one. The lagging distance has a marked influence on the

bending moments in the upper tunnel for both construction sequences. A slight decrease in the maximum bending moments in the lower tunnel when increasing the lagging distance is observed.

This study demonstrated the uplift behavior induced in the lower tunnel existing below the upper tunnel excavated following (scenarios 1, 2, and 3), and the supplementary settlement effect induced in the upper caused by the construction of the following lower tunnel (scenarios 4, 5, and 6). From a design point of view in terms of the tunnel lining stability and surface settlements, the results indicated that the critical scenario occurs when the upper tunnel is excavated first and is followed by the lower tunnel. In other words, the lower tunnel should be excavated first. On the other hand, the following upper tunnel should be excavated at a lagging distance L_F behind the preceding lower tunnel, which is larger by about 4D to 5D. At shorter lagging distances, increases in the bending moment, normal forces, and longitudinal forces in the twin tunnels are predicted. It is suggested to avoid designing too small pillar depth (B) between stacked tunnels, i.e., B values of 0.25D and 0.5D. This could cause an increment of the normal displacements, longitudinal forces, and bending moments in the lower tunnel lining.

It should be noted that the numerical investigation in the present study is conducted in drained conditions and for a homogeneous ground medium. Experimental studies and on-site monitoring will also be necessary in the future to validate the numerical results obtained in the study.

CRediT authorship contribution statement

Ngoc Anh Do: Conceptualization, Methodology, Software, Validation, Data curation, Writing – original draft, Writing – review & editing, Supervision, Project administration. **Daniel Dias:** Conceptualization, Methodology, Validation, Writing – review & editing, Supervision. **Mohammad-Reza Baghban Golpasand:** Investigation, Writing – review & editing. **Van Kien Dang:** Software, Data curation. **Ouahcène Nait-Rabah:** Software, Data curation. **Van Vi Pham:** Software, Data curation. **Trong Thang Dang:** Software, Validation, Data curation.

Declaration of Competing Interest

The authors declare that they have no known competing financial interests or personal relationships that could have appeared to influence the work reported in this paper.

Data availability

Data will be made available on request.

References

Addenbrooke, T.I., Potts, D.M., 2001. Twin tunnel interaction: surface and subsurface effects. Int. J. Geomech. 1 (2), 249–271.

Basile, F., 2014. Effects of tunnelling on pile foundations. Soils Found. 54 (3), 280–295.

Boon, C.W., Ooi, L.H., 2018. Longitudinal and transverse interactions between stacked parallel 7 tunnels constructed using shield tunneling in residual Soil. Geotech. Eng. J. SEAGS & AGSSEA 49 (2).

Channabasavaraj, W., Vishwanath, B., 2012. Influence of relative position of the tunnels - Numerical analysis on interaction between twin tunnels. In: Proceedings of Indian Geotechnical Conference, Delhi, pp. 500–503.

Chapman, D.N., Ahn, S.K., Hunt, D.VL., 2007. Investigating ground movements caused by the construction of multiple tunnels in soft ground using laboratory model tests. Can. Geotech. J. 44 (6), 631–643.

Chortis, F., Kavvadas, M., 2021. Three-dimensional numerical investigation of the interaction between twin tunnels. Geotech. Geol. Eng. https://doi.org/10.1007/s10706-021-01845-5.

Dias, D., Kastner, R., 2012. Movements caused by the excavation of tunnels using face pressurized shields - analysis of monitoring and numerical modelling results. Eng. Geol. 152 (1), 17–25.

Do, N.-A., Dias, D., Oreste, P., 2014a. Three-dimensional numerical simulation of mechanized twin stacked tunnels in soft ground. J. Zhejiang Univ. SCIENCE A 15 (11), 896–913.

Do, N.-A., Dias, D., Oreste, P., Djeran-Maigre, I., 2014b. Three-dimensional numerical simulation of a mechanized twin tunnels in soft ground. Tunnel. Undergr. Space Technol. 42, 40–51.

Do, N.-A., Dias, D., Oreste, P., Djeran-Maigre, I., 2014c. Three-dimensional numerical simulation for mechanized tunnelling in soft ground: the influence of the joint pattern. Acta Geotech. 9 (4), 673–694.

Do, N.A., Dias, D., Oreste, P.P., Djeran-Maigre, I., 2016. 3D Numerical investigation of mechanized twin tunnels in soft ground – influence of lagging distance between two tunnel faces. Eng. Struct. 109, 117–125.

Do, N.A., Dang, T.T., Dias, D., 2021. A numerical investigation of the impact of shield machine's operation parameters on the settlements above twin stacked tunnels - a case study of Ho Chi Minh urban railway Line 1 Vietnam. J. Earth Sci. 1–15 https://doi.org/10.15625/2615-9783/16442.

Epel, T., Mooney, M.A., Gutierrez, M., 2021. The influence of face and shield annulus pressure on tunnel liner load development. Tunnel. Undergr. Space Technol. 117, 104096. https://doi.org/10.1016/j.tust.2021.104096.

Fang, K., Yang, Z., Jiang, Y., Sun, Z., Wang, Z., 2020. Surface subsidence characteristics of fully overlapping tunnels constructed using tunnel boring machine in a clay stratum. Comput. Geotech. 125, 103679. https://doi.org/10.1016/j.compgeo.2020.103679.

Hage, C.F., Shahrour, I., 2008. Numerical analysis of the interaction between twin-tunnels: influence of the relative position and construction procedure. Tunnel. Undergr. Space Technol. 23, 210–214.

Hefny, A.M., Chua, H.C., Jhao, J., 2004. Parametric studies on the interaction between existing and new bored tunnels. Tunnel. Underground Space Technol. 19, 471.

Islam, S., Iskander, M., 2021. Twin tunneling induced ground settlements: a review. Tunnel. Undergr. Space Technol. 10, 103614 https://doi.org/10.1016/j.tust.2020.103614.

Itasca Consulting Group, 2013. FLAC Fast Lagrangian Analysis of Continua. User's manual.

Kim, S.H., 2004. Interaction behaviors between parallel tunnels in soft ground. Tunneling and Underground Space Technology. Underground space for sustainable urban development. Proceedings of the 30th ITA-AITES World Tunnel Congress Singapore.

Koungelis, D.K., Augarde, C.E., 2004. Interaction between multiple tunnels in soft ground, in Developments in mechanics of structures & materials: proceedings of the 18th Australasian Conference on the Mechanics of Structures and Materials, Perth, Australia, 1-3 December 2004. London: Taylor & Francis, pp. 1031-1036. Developments in mechanics of structures and materials, 2.

Li, X.G., Yuan, D.J., 2012. Response of a double-decked metro tunnel to shield driving of twin closely under-crossing tunnels. Tunn. Undergr. Space Technol. 28, 18–30.

Liu, Y., Fu, X., Yang, M., Tang, Z., Chen, L.u., Liu, Y., 2021. Numerical simulation study of overlapping tunnels in soft soil. IOP Conf. Series: Earth Environ. Sci. 634 (1), 012108. https://doi.org/10.1088/1755-1315/634/1/012108.

Loganathan, N., 2009. An innovative method for assessing tunnelling-induced risks to adjacent structures. Parsons Brinckerhoff Inc., One Penn Plaza New York, New York, p. 10119.

Mo, H.H., Chen, J.S., 2008. Study on inner force and dislocation of segments caused by shield machine attitude. Tunnel. Underground Space Technol. 23 (3), 281–291.

Mollon, G., Dias, D., Soubra, A.-H., 2012. Probabilistic analyses of tunneling-induced ground movements. Acta Geotech. 8 (2), 181–199.

Ng, C.W.W., Lee, K.M., Tang, D.K.W., 2004. Three-dimensional numerical investigations of new Austrian tunneling method (NATM) twin tunnel interactions. Cannadian Geotech. J. 41, 523–539.

Rijke, Q.C., 2006. Innovation of stress and damage reduction in bored tunnels during construction based on a shield equilibrium model. Ph.D. dissertation, Delft University of Technology and Holland Railconsult, Utrecht.

Senthilnath, G.T., Velu, D., 2016. Stacked tunneling induced surface settlements in soft soil – a case study from Singapore. Int. J. Geoeng. Case Histories 3 (3), 162–175.

Soomro, M.A., Kumar, M., Xiong, H., Mangnejo, D.A., Mangi, N., 2020. Investigation of effects of different construction sequences on settlement and load transfer mechanism of single pile due to twin stacked tunnelling. Tunn. Undergr. Space Technol. 96 (2020), 103171 https://doi.org/10.1016/j.tust.2019.103171.

Soomro, M.A., Kumar, M., Mangi, N., Mangnejo, D.A., Cui, Z.D., 2021a. Parametric Study of Twin Tunneling Effects on Piled Foundations in Stiff Clay: 3D Finite-Element Approach. Int. J. Geomech. https://doi.org/10.1061/(ASCE)GM.1943-5622.0002386.

Soomro, M.A., Mangi, N., Xiong, H., Kumar, M., Mangnejo, D.A., 2021b. Centrifuge and numerical modelling of stress transfer mechanisms and settlement of pile group due to twin stacked tunnelling with different construction sequences. Comput. Geotech. 121 (2020), 103449 https://doi.org/10.1016/j.compgeo.2020. 103449.

Surjadinata, J., Carter, J.P., Hull, T.S., Poulos, H.G., 2005. Analysis of effects of tunnelling on single piles. Conference: 5th International Symposium - Technical Committee TC28 at Amsterdam, Netherlands, Doi: 10.1201/b12748-93.

Tang, X., Gan, P., Li, J., Wang, H., 2016. Numerical analysis of reasonable spacing between tunnel faces during closely-spaced stacked tunneling. Electron. J. Geotech. Eng. 331–348.

Thienert, C., Pulsfort, M., 2011. Segment design under consideration of the material used to fill the annular gap. Geomech. Tunnel. 4, 665–679.

Yang, J., Liu, C., Chen, Q., Xie, X., 2017. Performance of overlapped shield tunneling through an integrated physical model tests, numerical simulations and real-time field monitoring. Underground Space 2 (1), 45–59.

Yamaguchi, I., Yamazaki, I., Kiritani, Y., 1998. Study of ground-tunnel interactions of four shield tunnels driven in close proximity, in relation to design and construction of parallel shield tunnels. Tunnel. Undergr. Space Technol. 13 (3), 289–304.

Yang, Z., Ding, Y., Jiang, Y., Fang, K., Dong, L., Qi, W., Wei, Z., 2020. Study of the construction sequence of overlapping tunnels by the shield tunneling method: a case study of the longest overlapping tunnel in China. Adv. Civil Eng. 2020, 1–9.

Zhang, H.J., Qiu, W.G., Feng, J.M., Zheng, Y.C., Gong, L., 2010. Study of longitudinal mechanical behavior and countermeasure for neighborhood overlapped shield tunneling. Rock Soil Mech. 31 (11), 3569–3573.

Zhang, W., Li, Y., Wu, C., Li, H., Goh, A.T.C., Liu, H., 2020. Prediction of lining response for twin tunnels constructed in anisotropic clay using machine learning techniques. Underground Space. https://doi.org/10.1016/j.undsp.2020.02.007.

Zhou, Z., Ding, H., Miao, L., Gong, C., 2021. Predictive model for the surface settlement caused by the excavation of twin tunnels. Tunneling Undergr. Space Technol. 114, 104014. https://doi.org/10.1016/j.tust.2021.104014.

Wang, H.N., Wu, L., Jiang, M.J., Song, F., 2017. Analytical stress and displacement due to twin tunneling in an elastic semi-infinite ground subjected to surcharge loads. Int. J. Numer. Anal. Meth. Geomech. 1–20 https://doi.org/10.1002/nag.2764.